amt-2014-320: Response to reviews

We are very grateful for the appraisals of this two-part study, particularly given the time required to assess both papers together. We thank the reviewers for their positive feedback and valuable suggestions for improving the manuscripts. All comments have been taken into account. Detailed responses to each point are provided below (in bold type), followed by the revised manuscript with the changes indicated.

Interactive comment on "Infrared and millimetre-wave scintillometry in the suburban environment – Part 1: Structure parameters" by H. C. Ward et al.

B. van Kesteren (Referee)

The authors present a two-part study in which they present the results of the first long-term application of an optical-microwave scintillometer system over Swindon, UK. In the first part, they present the results in terms of structure parameters and in the second part they present the results in terms of the heat fluxes.

Indeed, both manuscripts present research novel in many aspects. The application of a combined optical-microwave scintillometer system has been presented before, but never for such an extensive time period, nor over the city centre. This first part is addressing many technical issues at a high scientific level. They show strengths and weaknesses of all the scintillometric methods, as well as those of eddy-covariance measurements. On occasion the first manuscript points a bit too much towards the second manuscript to my opinion; the technical results and the results of the structure parameters already have value in themselves. Nevertheless, the manuscript is generally of a high scientific quality, presenting innovative results, and very well written, so that I recommend publication after minor revisions.

P 11171 – 17773, Introduction – the introduction gives a remarkably good overview of the state of the art in recent and older literature. Nevertheless, the part describing the objectives of this study (P 11173, line 24ff) is rather limited. To my opinion it does not get clear to readers who are not so familiar with the topic what this study contributes to the literature. It is stated that the presented dataset is "by far the longest dataset that uses these techniques", but it has not been stated yet, how long this period is. Furthermore, the sentence "Methodological considerations (…) and seasonality are explored" is rather vague and saying little. To my surprise, the conclusion, section 6, actually does a much better job in describing this relevance. Hence, the authors should make it more clear in the introduction already what this study contributes.

- **The length of the dataset (14 months) is now stated in the Introduction. The sentence beginning 'Methodological considerations…' has been deleted and the following text added to better describe the purpose of this paper: 'The performance of the techniques under different conditions, and their strengths and weaknesses, are examined. This paper offers insight into the behaviour of the structure parameters and r_{Tq} at various timescales (daily, seasonal and inter-annual), including how they respond to energy and water availability, surface cover and changing meteorological conditions.'**

P 11170, Line 9 – "unique", the use of this word is somewhat confusing here. It raises the thought that a rather exotic scintillometer is used, and with that the question on the representativeness of the results presented here. I would leave it out here.

- **'unique' has been deleted.**

P 11170, line 11-12 – "humidity fluctuations and the so-called", add a comma between "fluctuations" and "and".

- **Done.**

P 11170, line 12 – this sentence is hard to understand when one does not know the contents of the paper already. In itself the pairing of the two wavelengths already offers sensitivity to the humidity and temperature correlation. Mentioning the bi-chromatic method for this purpose is therefore unclear at this point when not introducing the two-wavelength method as well.

- **This has been rephrased as, 'the correlation between wavelengths is also used to retrieve the path-averaged temperature-humidity correlation'.**

P 11170, line 15 – to what does "the techniques" refer?

- **Changed to 'measurement techniques'.**

P 11170, line 20-21 – "The energy (…) companion paper.", it is unclear to me what this sentence is meant to say here, because you already introduced the companion paper before (line 9).

- **We refer back to the second paper at the end of the abstract to emphasise that this is a two-part study and the analysis (in terms of structure parameters in Part 1) continues (in terms of fluxes) in Part 2.**

P 11171, line 12 – "refraction", it results from diffraction. Rewrite.

- **Changed to 'diffraction'.**

P 11171, line 12 – introduce a semicolon after "beam" for readability

- **This sentence has been rewritten (see response to next point).**

P 11171, line 13 – the refractive index of an eddy is not determined by the density of constituent ones as is written here. Instead, the refractive index is defined as the factor with which the speed of an electromagnetic wave (speed of light, c) in a medium is reduced as compared to that in vacuum. Hence, the refractive index of an eddy is determined by the temperature and moisture content of the eddy itself. Rewrite.

- **This sentence has been rewritten as, 'Variations in the received intensity result from diffraction as turbulent eddies move through the beam, their refractive indices determined by their densities which, in turn, can be related to their temperature and moisture content (e.g. Meijninger 2003).'**

P 11171, line 17 – "humidity fluctuations are also important", writing it down like this suggests that temperature fluctuations are still important for millimetre or radiowaves, whereas their effect is rather limited. Rewrite

- **Changed 'also important' to 'more important'.**

P 11171, line 18 – "Peak sensitivity", sensitivity to what?

- **Changed to read 'Scintillometers are most sensitive to fluctuations occurring towards the centre of the path'.**

P 11171, line 21 – suggest to delete "other".

- **Done.**

P 11172, line 1-2 – "On the whole, (…) are-averaged fluxes.", how did these studies determine the blending height, that this conclusion can be drawn from them?

- **The common approach (to-date) to assess scintillometry fluxes is through comparison of area-averaged fluxes derived from scintillometry with fluxes from several eddy covariance stations aggregated to match the footprint of the scintillometer (e.g. Meijninger et al. (2002b), Ezzahar et al. (2007), Evans et al. (2012)). Ezzahar et al. (2007) conclude that scintillometry can be used below the blending height (a value of 26 m is stated). Their setup comprised two scintillometers installed below the blending height over an olive yard with patches of contrasting soil moisture. Estimates of the sensible heat flux and refractive index structure parameter derived from scintillometry and eddy covariance were compared. Meijninger et al. (2002b) used two scintillometers at different heights over mixed agricultural land and found better agreement with the higher scintillometer (installed above the blending height), but that the agreement with the lower scintillometer (sometimes below the blending height) could be improved by accounting for the composition of the footprint. Evans et al. (2012) found good agreement between fluxes from a scintillometer installed above the blending height and aggregated EC fluxes, also over mixed agriculture. In these latter two studies, the blending height was estimated following Wood and Mason (1991).**

P 11174, line 8, This definition of structure parameters in this line does not suffice. It perfectly applies to variances as well. However, in contrast to variances, the structure parameter is not dependent on the ensemble average of y(x), because the structure parameter considers, as Tatarskii expresses, only fluctuations smaller than the spatial separation δ. Rewrite.

- **For the purposes of the paper, the key point is that structure parameters are a measure of the strength of turbulent fluctuations (and they can be obtained from scintillometry and converted to fluxes via MOST). The sentence has been modified slightly to read, 'Structure parameters describe the intensity of turbulent fluctuations in the atmosphere.'**

P 11175, line 1-4 – AT and Aq are given in Ward et al. (2013b) as AT and Aq. I guess the latter instance of AT should be At? Otherwise the sentence makes no sense.

- **Thank you for the correction. This appears to be an error introduced in the typesetting. Yes, the text should read, '…given in Ward et al. (2013b) as A_t and A_q (see their Table 2).'**

P 11175, line 10 and Eq. (4). – "can be approximated", this formulation rightly suggest that the "="-sign in Eq. (4) should be replaced by an "≈"-sign.

- **Done.**

P 11175, line 13 – "typical atmospheric conditions". The question is: typical for where and when? Tropics? Swindon during summertime? Swindon during wintertime? Be more specific.

- **'(T = 300 K and pressure (p) = 10^5 Pa)' (Moene 2003) has been added to the text.**

P 11176, line 16 – put a comma after "method" and delete "obtained" for readability

- **Done.**

P 11177, line 1 – "most assumptions", what is meant with this? Maybe, "MOST assumptions"?

- **Thank you for the correction. This appears to be an error introduced in the typesetting. Yes, the text should read, 'If MOST assumptions'.**

P 11177, line 11 – this sentence is formulated somewhat confusing. I guess that plotting Cn2n2 versus β "reveals" the minimum, rather than letting it "occur".

- **Agreed: 'occurs' has been changed to 'is revealed'.**

P 11177, line 16-18 – "In practice, (…) of the instrument.", this sentence is vague. Please reformulate. So far as I get it, there is a region, where Cn2n2 is biased due to the bad SNR. Is that correct?

- **Yes, that appears to be the case. These sentences have been reworded as follows: 'In practice, zero C_{n2n2} will not be observed because the instrument has a finite noise floor (and $r_{Tq} \neq 1$). Instead the scintillation signal may be close to, or below, the detection limit of the instrument, resulting in reduced sensitivity around the region of minimum C_{n2n2} and a tendency for the derived β to be biased away from (below) the value at which minimum C_{n2n2} occurs.'**

P 11177, line 19ff – do the authors describe a new aspect of the above presented equations from "For low _, (…)" onwards? If not, then it is unclear to me how the Cn2n2 minimum relates to these last sentences.

- **These sentences have been moved earlier in the paragraph, after $S_{2\lambda}$ is first introduced.**

P 11179, line 20ff – METsub was installed at a height of 10m a.g.l. Could the authors elaborate whether these measurements were scaled to fit the scintillometer effective height?

- **Temperature, relative humidity and pressure were not scaled from the 10.6 m measurement height to the scintillometer effective height of 45.0 m. Sensitivity to these input variables has been shown to be small (Hartogensis et al. 2003; Ward et al. 2014b).**

Wind speed can be more important. The height of the wind speed measurement has been accounted for in the estimation of u_* for calculation of the fluxes.

P 11181, line 26 – σ^2_χ does not depict the covariance, maybe the authors can add $\sigma_{\chi 1\ \chi 2}$ (c.f. Eq. 14c)? Furthermore, the relation between the intensity measurements and the log-amplitude (co)variances does not become clear from this paper. I think it should be shown that var(ln(I)) = 0.25var(ln(χ)), or change it in the equations altogether.

- **This sentence has been modified to read, 'At 10-min intervals the variances, covariance and mean values of the signals were calculated, from which the log-amplitude variances ($\sigma^2_{\chi 1}$, $\sigma^2_{\chi 2}$) and covariance ($\sigma_{\chi 1 \chi 2}$) were obtained (Tatarski 1961).'**

P 11182, line 21-24 – "For the MWS (…) along the BLS-MWS path.", does fog also affect the MWS signal?

- **Although the MWS beam can propagate further through fog than the BLS beam, the 94 GHz signal is still affected by water droplets in the atmosphere. Rejection of data is based on signal intensity thresholds, so it is not known whether the inferred beam obscuration is due to rain or fog, or other matter (e.g. dust, birds). The decision was taken to remove MWS data at times when the BLS signal intensity suggested the optical beam was obscured to ensure that the resulting datasets are of high quality, i.e. to exclude times when variations in signal intensity may be due to processes other than scintillation.**

P 11182, line 27 – what do the authors mean with "reasonable thresholds"?

- **Data were excluded when $C_{n1n1} > 1.5 \times 10^{-14}$ m$^{-2/3}$; $C_{n2n2} > 1.5 \times 10^{-12}$ m$^{-2/3}$; $C_{n1n2} < -2.0 \times 10^{-13}$ m$^{-2/3}$ or $C_{n1n2} > 3.0 \times 10^{-13}$ m$^{-2/3}$. These thresholds were not explicitly given in the paper because they are fairly arbitrary, specific to this setup and the number of points outside these thresholds was very small (ten in total).**

P 11184, line 1 – could the authors elaborate on how well this methodology works during clouded weather or during winter time?

- **Using the positions of twice-daily minima in C_{n1n1} to mark a change of stability from unstable (daytime) to stable (night-time) generally worked well for this dataset. The transition times obtained are mostly similar to the transition times indicated by the EC station and the seasonal variation in identified transition times was as expected (i.e. more unstable hours in summer than winter). The EC data show that, for this suburban site, the atmosphere tends to be unstable during the day (although only for a short time around midday in winter) and stable at night (Ward et al. 2013a). Therefore, it is usually valid to assume there will be two stability transitions per day (at other sites this may not been the case and this methodology may not be suitable). The method was found to work less well in winter than summer as the transitions are often less well defined, stability can remain neutral (or close to neutral) throughout the day/night and there may be several transitions between slightly stable/slightly unstable conditions per day. Cloudy days were not usually problematic, although on a few occasions sudden cloud cover during sunny summer days led to a sharp dip in C_{n1n1} which were initially flagged erroneously as one of the minima indicating a stability transition. The algorithm was modified to include additional checks to**

handle these complications where possible. The cumulative daily net radiation was used to test if the minima identified could be due to sudden cloud cover; it was checked whether the positions of the identified minima were unrealistically close together; and time restrictions on the morning (after 0400) and evening (before 2100) transitions were imposed. If these checks were failed, the initial minimum identified was rejected and further minima were found.

- **The following text has been added to Section 5.1.1: 'Using the positions of C_{n1n1} minima to indicate the stability transition times generally worked well for this dataset, although performance was poorer in winter when stability changes tend to be less well defined and conditions may remain close to neutral throughout the day. Following the method described in Samain et al. (2012a), additional restrictions were imposed on the times of morning (here after 0400 UTC) and evening (before 2100 UTC) transitions. In a few cases, cumulative daily net radiation was also used to distinguish C_{n1n1} minima that were due to sudden cloud cover during daytime from C_{n1n1} minima that were due to a change of stability.'**

P 11185, line 14-15 – only experts will get what the authors imply here. I think they mean the path averaging over the licor and sonic sensors and their respective separation distance? Be more specific and give the corresponding references (Hill, 1991, Phys. Fluids A 3, 1572-1576 and Hartogensis, 2006).

- **This sentence has been modified to read, 'No corrections were made for spectral losses due to the spatial separation of the sonic and IRGA and their finite path lengths, which can be expected to result in underestimations of about 5–7% (Hill 1991; Hartogensis et al. 2002).'**

P 11186, line 4 – "sharp minima", sharp minima are not visible from the plots of figure 5a or 5b. The point the authors try to make in line 4-5, can only be illustrated when the corresponding figures have their y-axis logarithmically scaled. Hence, I would recommend to scale the y-axis of Fig 5a and 5b logarithmically, rather than linearly.

- **Figure 5a, b has been changed to a log scale.**

P 11188, line 9 – "means evaporation", these two words seem to interrupt the flow of the sentence and work confusing to me. I would recommend suitable punctuation for readability.

- **This has been rephrased as, 'In terms of fluxes, evapotranspiration continues throughout winter because moisture is readily available, whereas energy is limited so Q_H is directed towards the surface for much of the daytime, only becoming positive for a short time around midday (Ward et al. 2013a).'**

P 11190, line 20 – add a comma after "theory".

- **Done.**

P 11193, line 16-17 – recommend to rewrite "higher in the atmospheric boundary layer than is ideal," to read "to be above the surface layer,"

- **The text, 'likely higher in the atmospheric boundary layer than is ideal' has been changed to, 'possibly above the surface layer'.**

P 11193, line 19ff – Solignac (2012) indicates that high-pass filters may artificially reduce Cn2 at low crosswinds, i.e. cause underestimation of Cn2. To what extend do the authors think that their filter of 0.06 Hz affects the estimates of Cn2n2 and Cn1n2? This is an aspect that needs to be discussed at latest in this paragraph.

- **The suitability of different filter frequencies was investigated based on spectra and comparison of results (structure parameters and fluxes) for a range of different filter options. The value of 0.06 Hz used here is the same as that used by Lüdi et al. (2005). Altering this frequency slightly did not produce substantial changes to the results, whereas using much lower or higher frequencies was seen to impact both the spectra and magnitude of the results. The value of 0.06 Hz was therefore judged to be suitable for this dataset, but it is not critical that this exact value is used. Further research and development of a filter that varies according to atmospheric conditions (i.e. wind speed) may be an important area of future research. However, the poor performance at low crosswind speeds discussed in this paragraph could not be explained by the choice of filter frequency.**
- **The following text has been added to the end of the paragraph: 'Given that the position of the spectrum is known to change with wind speed (Medeiros Filho et al. 1983; Nieveen et al. 1998; Ward et al. 2011), and that C_n^2 can be underestimated if the filter excludes part of the scintillation signal under very low wind speed conditions (Solignac et al. 2012), the suitability of the bandpass filter was also re-examined. However, the choice of filter frequency did not seem to explain the poor performance and modifying the filter frequencies did not resolve the issues. Small changes in filter frequency generally did not produce substantial changes to the results, suggesting that the frequencies chosen are suitable for this dataset, but it is not critical that those exact values are used.'**

Another issue related to low crosswinds and recently analyzed in Lindenberg is the following: At low crosswind, the friction velocity usually is low as well, indicating that the inner scale length is large. Hill and Clifford (1978) indicate that D/l0 > 20 suffices for ignoring the spectral bump in the spectrum. Nevertheless, for the LITFASS set-up (4.8 km path, 43 m a.g.l.), a positive bias of Cn1n1, resulting from ignoring the l0-depenceof the spectrum, is as large as 30% for u* going to zero. The issue is described in more detail in Hartogensis (dissertation from 2006), appendix 5a. The effect of ignoring the bump on Cn1n2 and Cn2n2 is negligible. This information is just given here for consideration, and it would be great if the authors could elaborate their thoughts on it.

- **In urban environments, the friction velocity is rarely very small (due to the roughness of the surface and additional energy supply from anthropogenic activities); the EC data indicate $u_* < 0.1$ m s^{-1} for less than 3% of the dataset. The inner-scale effect is therefore expected to be relatively small for our setup, but we agree it may constitute another issue with the scintillometry technique at low (cross)wind speeds. This interesting topic would be a useful area for future study.**

P 11197, line 12 – add "of the first kind and zeroth and first order." After "Bessel functions".

- **‘of the first kind’ has been added after ‘Bessel functions’.**

P 11198, Eq. A1 – the term J0(K|d|) is only valid when the receivers and detectors of both scintillometers are identically separated at each side, otherwise the term should become J0(K|dt(1-x/L)+ dr(x/L)|), see Lüdi et al., Eq. (9) or Hill and Lataitis (1989) Eq. (1).

- ***d* is now defined as the beam separation.**

P 11198, line 6 – I recommend removing “is often applied”.

- **Modified accordingly.**

P 11198, line 11 – change “size of the Fresnel zone” to “maximal diameter of the first Fresnel zone”

- **Done.**

P 11198, line 11 – the variable “F” has not been defined before. Furthermore, I recommend giving its definition as well “F = √(λL)”

- **Done.**

Interactive comment on "Infrared and millimetre-wave scintillometry in the suburban environment – Part 1: Structure parameters" by H. C. Ward et al.

Anonymous Referee #2

Single review of both of the companion papers:

——————————- Overall comments / thoughts: ——————————

* A positive contribution to land-surface interactions, micro-meteorology, and scintillometry. This paper will certainly move science forward.

* Excellent quality figures (science and presentation).

* A very thorough work.

* In particular, Fig1 in the second paper is very important and nicely laid out.

* Language is almost flawless.

* It is a rare pleasure to review work of both high quality science and presentation.

———— Suggestions for improvements in general throughout the manuscripts: ————

* Can the uniqueness (a world first) of this work be more upfront, e.g. in the Highlights?

- **The Introduction has been modified to more clearly state the objectives and contributions of this work (please see responses to other comments).**

Some specific comments:

PAPER-A: ———

11172/6 » "derive" sounds exact/precise, maybe "estimate" is better.

- **'derive' has been changed to 'obtain'.**

11172/3 » Blending height and roughness sublayer are not well used in our field. Often there are two issues being combined. Can you make it clearer? (a) Blending height - we are thinking about averaging out horizontal heterogeneities (even for different surfaces of similar height). (b) Roughness sublayer is about considering differences in obstacle height (even for the same surface type). (See also other places in text)

- **The roughness sublayer describes the portion of the atmosphere directly surrounding the roughness elements (obstacles such as trees, buildings, etc) and extending from the surface up to a height of about $2z_H$ or more (Raupach et al. 1991). In the roughness sublayer, the flow is highly complex as it is distorted by the individual roughness elements.**
- **The concept of a blending height is used to describe the height above which the impact of surface heterogeneity is no longer important, i.e. where the influence of individual patches of different surface properties are averaged out, or blended together, by turbulent mixing.**

- **The term 'roughness sublayer' is not used in either paper but the blending height concept is now clarified in Section 3.1 ('i.e. high enough that turbulent mixing averages out the influence of surface heterogeneity').**

Table 1 » Do you need a column for z_H also?

- **Given that z_0 and z_d have been estimated from z_H by a simple multiplication, we decided not to include z_H in Table 1 as well.**

Figure 5 » Is a log scale needed here?

- **Figure 5a, b has been changed to a log scale.**

Figure 6 » The figure would be easier to interpret if something else like Q_H or Q* was plotted (or their sign), so one can see the transitions better.

- **Shading has been added to Figure 6 to indicate when Q^* > 0 W m^{-2}.**

PAPER-B: ———

- **Please see Part 2 response.**

Interactive comment on "Infrared and millimetre-wave scintillometry in the suburban environment – Part 2: Large-area sensible and latent heat fluxes" by H. C. Ward et al.

J.-M. Cohard (Referee)

H. Ward et al. present a paper series called "Infrared and millimetre-wave scintillometry in the suburban environment" containing 2 parts. – Part 1 is about the different ways to obtain structure parameters for temperature and specific humidity from scintillometers at different wave lengths. The part 2 is about the way to derive average turbulent fluxes from these structure parameters. The first part evaluates the performance of 3 methods, namely the single wave length method, the bichromatic method and the 2 wave length method. The second part develops objectively advantages and limitations of the scintillometry techniques. Both parts analyse a 14 months data time series obtained from july 2011 to December 2012 above Swindon (UK).

Theoretical backgrounds are clearly exposed highlighting the assumptions and limitations of the techniques deployed during this experiment. Results give a complete and detailed panorama of what is to be done when using Infra Red and Microwave scintillometers. It is based on the longest time series ever obtained for such technique. This huge amount of results and remarks will be very useful for any one wants to apply scintillometry techniques in the futur. Urban surface bowen ratios are finally presented and compared to previous studies. This last part will certainly require further analysis, but it is clearly not the main objective of these papers

Finally, this matches very well with the AMT journal and have to be published after minor corrections.

Some comments on both parts are listed below.

Part I : Structure parameters

p6 - 11174 L-18 : Add a reference (Hill 1981) for example.

- **Reference to Hill et al. (1980) has been added.**

p7 - 11175 L-10 : recall what the Bowen ratio is (QH/QLE). It is well known from most of us except if you want to address other community

- **To avoid confusion with Equation 9, the Bowen ratio is not explicitly given here in terms of fluxes.**

p12 - 11180 L 21 :Zd=0.7Zh is really not confirmed for open complex canopies. An estimation from EC data would be more appropriate. At least a remark on the reliability of this relation could be added given that this Zd parameter is recognize to be one of the most sensible for flux calculation from CT² values

- **Accurate estimates of the displacement height are difficult to obtain in complex environments, but the rule-of-thumb used here has also been used in other similar suburban areas. Moreover, the values obtained are within the range expected for similar environments (e.g. Grimmond and Oke 1999). Comparable values of z_d were estimated from the EC data for a reasonable range of z_0. In Part 2, Section 4.1.3, the impact on the fluxes of uncertainty in z_d is discussed and demonstrated to be unimportant given the**

considerable beam height ('The displacement height is incorporated in the effective height, and as a change in z_d of ±0.5 m is minor compared to z_{ef} itself, it has negligible impact (< 1 %) on the fluxes').

p12 - 11180 L 15 - 25 : Is this paragraph on equivalent height necessary to only compare Cn² values (what is done in this paper) ? For sure, you need to estimate Cn² values at compatible heights (EC and SC). As scintillometers provide good estimations of Cn² values, whereas EC Cn² are indirect estimations, I would prefer move the EC Cn² values from 12 to ....xx m (Explain in page 11184). In any case the difference in height from EC to scintillometer path should be discussed.

- **The effective height description here is part of the instrumental setup and is also needed for calculation of the S factors (see page 11183) which are used to scale the various scintillometer measurements to ensure they are representative of the same height (see Evans and De Bruin (2011) for details). The EC estimates of the structure parameters (C_T^2, C_q^2 and C_{Tq}) are indeed scaled to match the effective height of the scintillometer system for comparison (see page 11184 and Figures 7-9). In Figure 8, structure parameters from EC are plotted both before and after height scaling to match the scintillometer height; these results are discussed in Section 5.1.3.**

p15 - 11183 L15 : This is not a question of height but of weighting function. The diference in the equivalent height is a result of the integration of the weighting function. What it has to be accounted for is the difference in the way the Cn² values are averaged along the path. Don't forget that the sensor probe the same volume (more or less) at the same height.

- **Yes, the difference in path-weighting functions between the BLS and MWS means that the values of Cn1n1 and Cn2n2 (and Cn1n2) obtained are representative of different effective measurement heights. The wording has been modified to make this point clearer ('resulting from the combination of different weighting functions and changing beam elevation along the path').**

p15 - 11183 L25 : '3 techniques' appear not so clear to me as you just discussed 3 Cn² calculations but I understand you turn to a single, two wavelength and bichromatic method ....

- **Yes, that is correct.**

p16 - 11184 L11 : tau fixed at 1s . Does this can explain the weak correlation r_Tq found at night with EC data ? Please comment on that on page 11192 (if any answer !)

- **The nocturnal r_{Tq} values are fairly similar for different wind speeds and there is no clear indication that the values of r_{Tq} obtained are dependent on wind speed. Therefore the fixed time lag does not seem to explain the weak correlation. The spatial separation of the sonic and IRGA is probably responsible for the magnitude of r_{Tq} being underestimated. However, other studies have also indicated that absolute values of r_{Tq} are smaller at night than during the day. For example r_{Tq} was found to range between -0.5 and 0.9 (Meijninger et al. 2006) and Lüdi et al. (2005) find that the T-q anti-correlation at night is 'less pronounced' than the positive correlation during daytime. The following sentence has been added to the discussion in Section 5.2, 'According to Lüdi et al. (2005) the T-q anti-**

correlation observed at night is 'less pronounced' than the positive correlation during daytime; Meijninger et al. (2006) also found r_{Tq} ranged between -0.5 and 0.9.'

p19 - 11187 : line 19 and after please, use the same subscript code along the paper. you have define the substrict 1l, 2l and bc. just use it. If a SC is necessary to invite the reader considering all of the three techniques, define it. The BLS_MWS notation is quite long and "heavy".

- **We agree the BLS-MWS subscript is fairly cumbersome, however it represents exactly what we wish to convey – quantities derived from the BLS-MWS system, using either the two-wavelength or bichromatic technique (but not the single-wavelength technique). We would therefore prefer to continue using BLS-MWS, rather than introduce yet more notation.**

p19 - 11187 : L19 -23 : Finally this paragraph say not so much. I would replace it with a clear invitation to the part II (1 sentence)

- **Done. The first two sentences have been deleted and the sentence referencing Part 2 has been moved to the end of the previous paragraph.**

p22 - 11190 : L1 ... this discussion on Bowen ratio should better take place around line 8 in page 11188. However as you mentioned it, the analysis of Beta will be easier with the fluxes. I suggest suppressing this paragraph and replacing it by extended comments on the differences between Beta_EC and Beta_SC (footprint differences, height differences, Beta calculation from SC and EC, the latest is not précised. Is it w'T'/w'q' or is it calculated with Eq 9, statistical issues ?). At least the Beta curves show few Beta differences using the 2 wavelength or the bichromatic method …b ut is these estimates reliable? (Half the EC value!!)

More over the Beta estimates you mentioned in the text (Beta_2lambda < 1.3) doesn't match with what is plotted in figure 9 where these values are always under 0.5. Please clarify. Finally, you conclude (in the conclusion) the differences came from footprint differences, but this has not been discussed here.

- **The discussion on Bowen ratios in Section 5.1.4 has now been moved to the end of Section 5.1.3.**
- **The mean daytime Bowen ratio for each month is plotted in Figure 9. β was calculated from Equation 9 (this is now stated in the figure caption). The individual 10-min or 30-min values are spread around these means, and they vary both throughout the day and between days as the meteorological and surface conditions vary. It is these individual $\beta_{\_2\lambda}$ values that appear to be limited to ≤ 1.3. The fact that the BLS-MWS footprint is more vegetated than the EC footprint is also mentioned here now.**

p23 -n11191 : The r_Tq plateau at 1 is a rough approximation. I would precise this (0.8?) r_Tq for low wind speed (the same eddy can be probe several time which increase the correlation. Pb of the inversion for noisy data.

- **'close to +1' has been changed to 'around 0.8'.**
- **We are unsure of the meaning of 'Pb of the inversion for noisy data'.**

p27 11195 : The conclusion could be shorter. It is not necessary to recall equation (L 6 - 15). It could be re organized starting from the technical insights (appendix), the CT^2 Cq^2, ... consistency, r_Tq, Bowen ratio and method comparison.

Considering this conclusion, I would also reorganise the discussion to point out the different argumentations that lead to these conclusion (Like the one I have suggested for Beta).

- **The references to the appendix and equation have been deleted.**
- **Methodological differences as well as footprint differences (now mentioned in Section 5.1.3) are given as explanations for the observed differences in Bowen ratio.**

fig 4 precise somewhere how the spectra has been calculated (windowing, ...) especially for the black line. I guess the grey line is a direct calculation (rectangular window) over the 30 min segment and I suspect the black line to be a bin average.

- **Yes, the grey line is a direct calculation over the 30-min rectangular window; the black line is the smoothed spectrum (bin averages for the data divided into 100 bins). This is now mentioned in the Figure caption.**

fig 8 : I suspect an error in the axes legend r_EC_bc in place or r_Tq ? More over the color line legend is missing in the figure and in the legend. It is also not clear to me on how these correlations have been calculated: 30min OK but with min data ?

- **The panels in the bottom row of Figure 8 show r_{Tq} calculated from EC (black) and r_{Tq} calculated from the bichromatic method (green). The legend is shown in the top right-hand panel and is the same for all panels. Meteorological structure parameters for the single-wavelength, two-wavelength and bichromatic-correlation methods were obtained at 10-min intervals from the 10-min refractive index structure parameters (Section 3.2.1). Due to the variability of the bichromatic method, the 10-min meteorological structure parameters were averaged up to 30-min. r_{Tq_bc} was then calculated from these 30-min structure parameters.**

Part II : Large-area sensible and latent heat fluxes

- **Please see Part 2 response.**

References

Evans JG and De Bruin HAR (2011) The Effective Height of a Two-Wavelength Scintillometer System. Boundary-Layer Meteorol 141: 165-177. doi: 10.1007/s10546-011-9634-0

Evans JG, McNeil DD, Finch JW, Murray T, Harding RJ, Ward HC and Verhoef A (2012) Determination of turbulent heat fluxes using a large aperture scintillometer over undulating mixed agricultural terrain. Agric For Meteorol 166-167: 221-233.

Ezzahar J, Chehbouni A and Hoedjes JCB (2007) On the application of scintillometry over heterogeneous grids. J Hydrol 334: 493-501. doi: 10.1016/j.jhydrol.2006.10.027

Grimmond CSB and Oke TR (1999) Aerodynamic properties of urban areas derived from analysis of surface form. J Appl Meteorol 38: 1262-1292.

Hartogensis OK, De Bruin HAR and Van De Wiel BJH (2002) Displaced-Beam Small Aperture Scintillometer Test. Part Ii: Cases-99 Stable Boundary-Layer Experiment. Boundary-Layer Meteorol 105: 149-176. doi: 10.1023/a:1019620515781

Hartogensis OK, Watts CJ, Rodriguez JC and De Bruin HAR (2003) Derivation of an effective height for scintillometers: La Poza experiment in Northwest Mexico. J Hydrometerol 4: 915-928.

Hill RJ (1991) Comparison of experiment with a new theory of the turbulence temperature structure-function. Physics of Fluids a-Fluid Dynamics 3: 1572-1576. doi: 10.1063/1.857936

Hill RJ, Clifford SF and Lawrence RS (1980) Refractive-index and absorption fluctuations in the infrared caused by temperature, humidity, and pressure fluctuations. J Opt Soc Am 70: 1192-1205.

Lüdi A, Beyrich F and Matzler C (2005) Determination of the turbulent temperature-humidity correlation from scintillometric measurements. Boundary-Layer Meteorol 117: 525-550. doi: 10.1007/s10546-005-1751-1

Medeiros Filho F, Jayasuriya D, Cole R and Helmis C (1983) Spectral density of millimeter wave amplitude scintillations in an absorption region. Antennas and Propagation, IEEE Transactions on 31: 672-676.

Meijninger WML, Beyrich F, Lüdi A, Kohsiek W and De Bruin HAR (2006) Scintillometer-based turbulent fluxes of sensible and latent heat over a heterogeneous land surface - A contribution to LITFASS-2003. Boundary-Layer Meteorol 121: 89-110. doi: 10.1007/s10546-005-9022-8

Meijninger WML, Hartogensis OK, Kohsiek W, Hoedjes JCB, Zuurbier RM and De Bruin HAR (2002) Determination of area-averaged sensible heat fluxes with a large aperture scintillometer over a heterogeneous surface - Flevoland field experiment. Boundary-Layer Meteorol 105: 37-62.

Moene AF (2003) Effects of water vapour on the structure parameter of the refractive index for near-infrared radiation. Boundary-Layer Meteorol 107: 635-653.

Nieveen JP, Green AE and Kohsiek W (1998) Using a large-aperture scintillometer to measure absorption and refractive index fluctuations. Boundary-Layer Meteorol 87: 101-116.

Raupach MR, Antonia RA and Rajagopalan S (1991) Rough-Wall Turbulent Boundary Layers. Applied Mechanics Reviews 44: 1-25.

Samain B, Defloor W and Pauwels VRN (2012) Continuous Time Series of Catchment-Averaged Sensible Heat Flux from a Large Aperture Scintillometer: Efficient Estimation of Stability Conditions and Importance of Fluxes under Stable Conditions. J Hydrometerol 13: 423-442. doi: 10.1175/jhm-d-11-030.1

Solignac PA, Brut A, Selves JL, Béteille JP and Gastellu-Etchegorry JP (2012) Attenuating the Absorption Contribution on {C_{n^{2}}} Estimates with a Large-Aperture Scintillometer. Boundary-Layer Meteorol 143: 261-283. doi: 10.1007/s10546-011-9692-3

Tatarski VI (1961) Wave Propagation in a Turbulent Medium, McGraw-Hill, New York, 285 pp

Ward HC, Evans JG and Grimmond CSB (2011) Effects of Non-Uniform Crosswind Fields on Scintillometry Measurements. Boundary-Layer Meteorol 141: 143-163. doi: 10.1007/s10546-011-9626-0

Ward HC, Evans JG and Grimmond CSB (2013a) Multi-season eddy covariance observations of energy, water and carbon fluxes over a suburban area in Swindon, UK. Atmos Chem Phys 13: 4645-4666. doi: 10.5194/acp-13-4645-2013

Ward HC, Evans JG and Grimmond CSB (2014) Multi-scale sensible heat fluxes in the urban environment from large aperture scintillometry and eddy covariance. Boundary Layer Meteorol 152: 65-89. doi: 10.1007/s10546-014-9916-4

Ward HC, Evans JG, Hartogensis OK, Moene AF, De Bruin HAR and Grimmond CSB (2013b) A critical revision of the estimation of the latent heat flux from two-wavelength scintillometry. Q J R Meteorol Soc 139: 1912-1922. doi: 10.1002/qj.2076

Wood N and Mason P (1991) The influence of static stability on the effective roughness lengths for momentum and heat transfer. Q J R Meteorol Soc 117: 1025-1056. doi: 10.1002/qj.49711750108

Infrared and millimetre-wave scintillometry in the suburban environment – Part 1: structure parameters

H.C. Ward[1, 2, 3], J.G. Evans[1], C.S.B. Grimmond[2, 3] and J. Bradford[4]

[1] Centre for Ecology and Hydrology, Wallingford, Oxfordshire, UK, OX10 8BB
[2] Department of Geography, King's College London, London, UK, WC2R 2LS
[3] Department of Meteorology, University of Reading, Reading, RG6 6BB, UK
[4] Space Science Department, Rutherford Appleton Laboratory, Didcot, Oxfordshire, UK, OX11 0QX

Corresponding author email: h.c.ward@reading.ac.uk

Abstract

Scintillometry, a form of ground-based remote sensing, provides the capability to estimate surface heat fluxes over scales of a few hundred metres to kilometres. Measurements are spatial averages, making this technique particularly valuable over areas with moderate heterogeneity such as mixed agricultural or urban environments. In this study, we present the structure parameters of temperature and humidity, which can be related to the sensible and latent heat fluxes through similarity theory, for a suburban area in the UK. The fluxes are provided in the second paper of this two-part series. A ~~unique~~ millimetre-wave scintillometer was combined with an infrared scintillometer along a 5.5 km path over northern Swindon. The pairing of these two wavelengths offers sensitivity to both temperature and humidity fluctuations, and the ~~so-called 'bichromatic-correlation' method~~correlation between wavelengths is also used to retrieve the path-averaged temperature-humidity correlation. Comparison is made with structure parameters calculated from an eddy covariance station located close to the centre of the scintillometer path. The performance of the measurement techniques under different conditions is discussed. Similar behaviour is seen between the two datasets at sub-daily timescales. For the two summer-to-winter periods presented here, similar evolution is displayed across the seasons. A higher vegetation fraction within the scintillometer source area is consistent with the lower Bowen ratio observed (midday Bowen ratio < 1) compared with more built-up areas around the eddy covariance station. The energy partitioning is further explored in the companion paper.

Keywords: bichromatic correlation; refractive index; temperature-humidity correlation; two-wavelength scintillometry; urban

Highlights

- First use of two-wavelength scintillometry in an urban area
- Temperature-humidity correlation coefficient measured by bichromatic-correlation
- Performance of techniques assessed under a range of conditions
- Extensive dataset enables analysis of seasonal and inter-annual variability

1. Introduction

Scintillometry provides turbulent heat fluxes representative of much larger scales than is possible with traditional point-based or small-area measurements, such as eddy covariance (EC). The technique relates fluctuations in the intensity of light (‘scintillations’, observed as shimmering or ‘heat-haze’) to the strength of turbulence in the atmosphere. Scintillometry is suited to heterogeneous regions because the measurements are spatially integrated, providing average values representative of the area as a whole (Hoedjes et al. 2002; Meijninger et al. 2002b; Evans et al. 2012). A transmitter unit provides the light source, a beam of electromagnetic radiation, which is detected some distance (0.1-10 km) away by the receiver. Variations in the received intensity result from ~~refraction~~ diffraction as turbulent eddies move through the beam, their refractive indices determined by their densitiesy ~~of constituent air parcels~~ which, in turn, can be related to their temperature and moisture content (e.g. Meijninger 2003). The refractive index depends on the wavelength of radiation; in the optical or near-infrared range temperature-induced fluctuations dominate the refractive index fluctuations, whereas for longer wavelengths (millimetre or radiowave regions) humidity fluctuations are ~~also~~ more important. ~~Peak sensitivity is~~ Scintillometers are most sensitive to fluctuations occurring towards the centre of the path, i.e. away from the transmitter and receiver and their mountings. Thus the atmosphere above a city (or valley) can be sampled remotely – a major advantage in areas where it would be impracticable to install ~~other~~ equipment *in situ*.

Scintillometer measurements have been carried out at sites of varying complexity, from tests of the technique under simple conditions (Hill and Ochs 1978; De Bruin et al. 1993) to studies investigating the complications of non-ideal terrain, including heterogeneous land cover (Beyrich et al. 2002; Meijninger et al. 2002a; Meijninger et al. 2006; Ezzahar et al. 2007) and complex topography (Poggio et al. 2000; Evans 2009; Evans et al. 2012). On the whole, these studies have shown that scintillometers installed above or close to the blending height can provide valuable area-averaged fluxes.

With careful selection of a suitable path, the scintillometry technique has been successfully used in urban areas. Kanda et al. (2002), the first to derive obtain the sensible heat flux in an urban setting, used two small aperture scintillometers installed at different heights on a 250 m path over a dense residential area of Tokyo. Other small aperture studies include measurements in Basel (Roth et al. 2006) and London (Pauscher 2010). Large aperture scintillometers are increasingly being used over longer urban paths (Lagouarde et al. 2006; Gouvea and Grimmond 2010; Mestayer et al. 2011; Wood et al. 2013; Zieliński et al. 2013). These infrared (or optical) scintillometers must rely on the residual of the energy balance if the latent heat flux is to be estimated. However, the complexity of the energy balance (Oke 1987) means this is usually not attempted in urban areas. In particular the significant storage heat flux (Oke et al. 1999; Offerle et al. 2005) and contribution from anthropogenic activities (Klysik 1996; Allen et al. 2011) are both very difficult to measure.

Sensitivity to both humidity and temperature fluctuations can be achieved with a two-wavelength scintillometer system. In this case, the structure parameter of humidity can be obtained in addition to the structure parameter of temperature, from which both the sensible heat flux (Q_H) and latent heat flux (Q_E) can be found (Hill et al. 1988; Andreas 1989). Several studies have reported successful estimates of Q_E using the two-wavelength method (Meijninger et al. 2002a; Meijninger et al. 2006; Evans 2009; Evans et al. 2010). This technique requires that a value of the temperature-humidity correlation coefficient, r_{Tq}, be assumed. Often r_{Tq} is taken to be ±1, indicating perfect correlation, as in Green et al. (2001) and Meijninger et al. (2002a), but other values have also been used: Kohsiek and Herben (1983) used r_{Tq} = 0.87; Evans (2009) used r_{Tq} = 0.8; and Meijninger et al. (2006) used measured r_{Tq} from a nearby EC station with values between -0.5 and 0.9. Previous studies measuring r_{Tq} with fast-response sensors suggest daytime values tend to be smaller than 1, typically around 0.8. For example: 0.75 at a flat, homogeneous site (Kohsiek 1982); 0.76 over sandy soil with patchy vegetation (Andreas et al. 1998); 0.70-0.95 for unstable conditions over heterogeneous farmland (Meijninger et al. 2002a). Nocturnal values of r_{Tq} down to -1 are rarely seen (Andreas et al. 1998; Beyrich et al. 2005; Meijninger et al. 2006).

Some studies have suggested that r_{Tq} varies with stability (Li et al. 2011; Nordbo et al. 2013), although others have shown no clear relation (De Bruin et al. 1993; Roth 1993). Explanation of $|r_{Tq}| \neq 1$ is often related to surface heterogeneity (Roth 1993; Andreas et al. 1998; Lüdi et al. 2005) but low values have been obtained over homogeneous surfaces too (Kohsiek 1982; De Bruin et al. 1993). In almost all previous studies, measurements of r_{Tq} were made using point sensors.

Lüdi et al. (2005) outlined a method to obtain path-averaged values of r_{Tq} using a two-wavelength scintillometer system. This ‘bichromatic-correlation’ method is an extension of the two-wavelength technique and involves correlating the signals from each scintillometer, thus enabling determination of the combined temperature-humidity fluctuations and r_{Tq}. The bichromatic-correlation method, applied for the first time during the LITFASS-2003 campaign, gave promising results (Beyrich et al. 2005; Lüdi et al. 2005). An overview of the second study, during LITFASS-2009, is given in Beyrich et al. (2012).

Aside from enabling more accurate structure parameters and fluxes to be obtained from scintillometry, improved knowledge of r_{Tq} has wider applications. Correlations between scalars are thought to be useful indicators for the violation of Monin-Obukhov Similarity Theory (MOST) (Hill 1989; Andreas et al. 1998). Correlations are also relevant to the understanding and modelling of turbulent transport processes through physical quantities such as eddy diffusivities.

The objectives of this research are to measure structure parameters and obtain large-area sensible and latent heat fluxes for a suburban area. In this two-part study, a 94 GHz millimetre-wave scintillometer was deployed alongside an infrared scintillometer over the town of Swindon, UK. This is the first use of such a system in the urban environment. In Part 1, structure parameters from the two-wavelength system are compared to structure parameters calculated from an EC system and measured values of r_{Tq} are discussed. In Part 2, the sensible and latent fluxes are determined and analysed (Ward et al. 2014a). These spatially-integrated observations represent the behaviour of the suburban surface over an area of 5-10 km^2 and constitute by far the longest dataset (14 months) that uses these techniques. ~~Methodological considerations, the~~ The performance of the techniques under different conditions, and their strengths and weaknesses, are examined. This paper offers insight into the behaviour of the structure parameters and r_{Tq} at various timescales (daily, seasonal and inter-annual), ~~and~~ including how they respond to ~~the influence of~~ energy and water availability, surface cover and changing meteorological conditions ~~vegetation cover and seasonality are explored~~.

2. Theory

Structure parameters describe the intensity of turbulent fluctuations in the ~~turbulent~~ atmosphere. The structure parameter for a variable, y, is defined (Tatarski 1961),

$$C_y^2 = \frac{\overline{[y(x+\delta)-y(x)]^2}}{\delta^{2/3}}, \tag{1}$$

where δ is the spatial separation between two points and $y(x)$ is the value of the variable at location x. The cross-structure parameter between two variables is defined analogously, for example the cross-structure parameter between temperature, T, and specific humidity, q, is written,

$$C_{Tq} = \frac{\overline{[T(x+\delta)-T(x)][q(x+\delta)-q(x)]}}{\delta^{2/3}}. \tag{2}$$

2.1. Obtaining structure parameters from scintillometry

The refractive index structure parameter (C_n^2) is fundamental to scintillometry. For each wavelength, λ, it can be written (Hill et al. 1980),

$$C_n^2 = \frac{A_T^2}{T^2} C_T^2 + 2\frac{A_T A_q}{Tq} C_{Tq} + \frac{A_q^2}{q^2} C_q^2, \tag{3}$$

where C_T^2 is the structure parameter of temperature, C_q^2 the structure parameter of specific humidity, C_{Tq} the temperature-humidity cross-structure parameter and A_T and A_q are the structure parameter coefficients for temperature and specific humidity respectively, given in Ward et al. (2013b) as A_t and A_q (see their Table 2). These coefficients contain the wavelength dependence of C_n^2, whereas C_T^2, C_q^2 and C_{Tq} are properties of the atmosphere. Each C_n^2 measurement is made up of a combination of the three unknowns: C_T^2, C_q^2 and C_{Tq}.

As C_n^2 from large aperture optical or near-infrared scintillometers is almost entirely made up of temperature fluctuations (C_T^2), the (usually small) contributions from C_{Tq} and C_q^2 can be approximated using the Bowen ratio, β (Wesely 1976; Moene 2003):

$$C_n^2 \approx \frac{A_T^2}{T^2} C_T^2 \left(1 + \frac{A_q}{q}\frac{T}{A_T}\frac{c_p}{L_v}\beta^{-1}\right)^2 \approx \frac{A_T^2}{T^2} C_T^2 \left(1 + 0.03\beta^{-1}\right)^2, \tag{4}$$

where c_p is the specific heat capacity of air at constant pressure, L_v is the latent heat of vaporisation and the value 0.03 is for typical atmospheric conditions (T = 300 K, pressure (p) = 10^5 Pa). The required Bowen ratio may be found by using the available energy as an input to the iteration to obtain the sensible heat flux (e.g. Green and Hayashi 1998; Meijninger et al. 2002b; Solignac et al. 2009). Calculation of the latent heat flux must rely on the energy balance (Ezzahar et al. 2009; Guyot et al. 2009; Evans et al. 2012; Samain et al. 2012b). This is the single-wavelength scintillometry method.

As demonstrated by Hill et al. (1988) and Andreas (1989), a two-wavelength scintillometer system enables retrieval of both C_T^2 and C_q^2 via simultaneous equations (Equation 3 for each wavelength). The two-wavelength method has the significant advantage of providing both sensible and latent heat fluxes without resorting to the energy balance, but a value for the temperature-humidity correlation coefficient r_{Tq} must be assumed in the substitution $C_{Tq} = r_{Tq}(C_T^{\,2}C_q^{\,2})^{1/2}$.

The bichromatic-correlation method uses the same combination of optical and millimetre wavelength scintillometers as for the two-wavelength method, but additionally exploits the correlation between optical and millimetre-wave signals to obtain a third equation for the cross-structure parameter, C_{n1n2} (Lüdi et al. 2005),

$$C_{n1n2} = \frac{A_{T1}A_{T2}}{T^2}C_T^2 + \left(\frac{A_{T1}A_{q2} + A_{T2}A_{q1}}{Tq}\right)C_{Tq} + \frac{A_{q1}A_{q2}}{q^2}C_q^2, \tag{5}$$

where the subscripts 1 and 2 refer to the different wavelengths. In this study, λ_1 denotes optical (specifically 880 × 10^{-9} m) and λ_2 millimetre (3.2 × 10^{-3} m) wavelengths. Thus all three unknown meteorological structure parameters (C_T^2, C_q^2 and C_{Tq}) can be found from the three measured refractive index structure parameters by inverting the matrix equation (Lüdi et al. 2005),

$$(C_{n1n1} \quad C_{n2n2} \quad C_{n1n2}) = \mathbf{M}\begin{pmatrix} C_T^2 \\ C_{Tq} \\ C_q^2 \end{pmatrix}, \tag{6}$$

where the inverse matrix $\mathbf{M}^{-1}$ is given by,

$$\mathbf{M}^{-1} = \frac{T^2q^2}{(A_{T1}A_{q2} - A_{T2}A_{q1})^2}\begin{pmatrix} \dfrac{A_{q2}^{\;2}}{q^2} & \dfrac{A_{q1}^{\;2}}{q^2} & \dfrac{-2A_{q1}A_{q2}}{q^2} \\ \dfrac{-A_{T2}A_{q2}}{Tq} & \dfrac{-A_{T1}A_{q1}}{Tq} & \dfrac{(A_{T1}A_{q2} + A_{T2}A_{q1})}{Tq} \\ \dfrac{A_{T2}^{\;2}}{T^2} & \dfrac{A_{T1}^{\;2}}{T^2} & \dfrac{-2A_{T1}A_{T2}}{T^2} \end{pmatrix}. \tag{7}$$

As mentioned above, the structure parameter coefficients A_T and A_q should be those formulated using specific humidity.

For the bichromatic-correlation method, the value of C_{Tq} ~~obtained~~ can therefore be used to effectively measure the temperature-humidity correlation coefficient:

$$r_{Tq} = \frac{C_{Tq}}{\sqrt{C_T^2 C_q^2}} . \tag{8}$$

If MOST assumptions (i.e. T-q similarity) are satisfied, the Bowen ratio can be calculated from the structure parameters (Andreas 1990; Lüdi et al. 2005),

$$\beta = \mathrm{sgn}[C_{Tq}] \frac{c_p}{L_v} \sqrt{\frac{C_T^2}{C_q^2}} . \tag{9}$$

When the cross-structure parameter has not been measured, the structure parameters C_T^2 and C_q^2 can be calculated from the two-wavelength equations, after Hill et al. (1988):

$$C_T^2 = \frac{A_{q2}^2 C_{n1n1} + A_{q1}^2 C_{n2n2} + 2 r_{Tq} A_{q1} A_{q2} S_{2\lambda} \sqrt{C_{n1n1} C_{n2n2}}}{(A_{T1} A_{q2} - A_{T2} A_{q1})^2 T^{-2}} , \tag{10a}$$

$$C_q^2 = \frac{A_{T2}^2 C_{n1n1} + A_{T1}^2 C_{n2n2} + 2 r_{Tq} A_{T1} A_{T2} S_{2\lambda} \sqrt{C_{n1n1} C_{n2n2}}}{(A_{T1} A_{q2} - A_{T2} A_{q1})^2 q^{-2}} , \tag{10b}$$

where $S_{2\lambda}$ is ±1. This choice of sign is an inherent ambiguity of the two-wavelength method and represents two possible solutions to C_{n2n2} (Hill et al. 1988; Hill 1997). For low β, when humidity fluctuations dominate C_{n2n2} then $S_{2\lambda}$ = +1, whereas $S_{2\lambda}$ = -1 is required at larger β. The sign of $S_{2\lambda}$ is not known *a priori* but must be assumed. Often the two solutions for β indicate which is the most likely solution for the atmospheric conditions and site characteristics (Hill 1997). When expressed as a function of β, a minimum in C_{n2n2} ~~occurs~~ is revealed due to the coefficients A_T and A_q having opposite signs at millimetre wavelengths. The contribution of C_{Tq} to C_{n2n2} (middle term in Equation

3) is negative when $C_{Tq} > 0$, so for moderate β the terms in Equation 3 can cancel out leaving C_{n2n2} close to zero (Hill et al. 1988; Otto et al. 1996). ~~In practice, a finite instrumental noise floor (and $r_{Tq} \neq 1$) means zero C_{n2n2} will not be observed. Instead a measurement problem of reduced sensitivity is created around the region of minimum C_{n2n2}, where the scintillation signal may be close to, or below, the detection limit of the instrument.~~ In practice, zero C_{n2n2} will not be observed because the instrument has a finite noise floor (and $r_{Tq} \neq 1$). Instead the scintillation signal may be close to, or below, the detection limit of the instrument, resulting in reduced sensitivity around the region of minimum C_{n2n2} and a tendency for the derived β to be biased away from (below, for $S_{2\lambda} = +1$) the value at which minimum C_{n2n2} occurs. The problematic region is expected to occur for $\beta \approx 2$-3 (Leijnse et al. 2007; Ward et al. 2013b). ~~For low β, when humidity fluctuations dominate C_{n2n2} then $S_{2\lambda} = +1$, whereas $S_{2\lambda} = -1$ is required at larger β. The sign of $S_{2\lambda}$ is not known *a priori* but must be assumed. Often the two solutions for β indicate which is the most likely solution for the atmospheric conditions and site characteristics (Hill 1997).~~

2.2. Obtaining structure parameters from eddy covariance

Conversion between spatial and temporal domains enables calculation of structure parameters from point measurements, such as those from EC instrumentation. The spatial structure function, D_{yy_x}, can be written (e.g. Stull 1988),

$$D_{yy\_x}(\delta) = \overline{[y(x+\delta) - y(x)]^2} \ . \tag{11}$$

Analogously the temporal structure function, D_{yy_t}, is given by,

$$D_{yy\_t}(\tau) = \overline{[y(t+\tau) - y(t)]^2} \ , \tag{12}$$

where τ is the temporal separation and $y(t)$ is the value of the variable at time t. Bosveld (1999) gives the conversion between temporal and spatial structure functions using the horizontal wind vector, U, and the variances of the three wind components, $\sigma^2_{u,v,w}$:

$$D_{yy\_x}(\delta) = \frac{D_{yy\_t}(\delta / U)}{\left(1 - \frac{1}{9}\frac{\sigma_u^2}{U^2} + \frac{1}{3}\frac{\sigma_v^2}{U^2} + \frac{1}{3}\frac{\sigma_w^2}{U^2}\right)}. \quad (13)$$

Thus temporal structure functions (Equation 12) can be calculated from EC measurements, converted to spatial structure functions (Equation 13) and then structure parameters ($C_y^2 = D_{yy\_x}(\delta)\ \delta^{-2/3}$ defines C_y^2 for δ in the inertial subrange). Unlike fluxes, structure parameters are strongly height dependent.

3. Experimental details

3.1. Instrumental setup and site description

A unique millimetre-wave scintillometer (MWS) (Evans 2009), designed and built by the Centre for Ecology and Hydrology (CEH) and Rutherford Appleton Laboratory (RAL), was used in combination with a commercially available large aperture infrared scintillometer, the BLS900 (Scintec, Rottenburg, Germany). Both scintillometers were installed on a 5.5 km path over the town of Swindon, UK. The path is orientated approximately north-south (170°) and extends from the edge of the settlement to the town centre (Figure 1). An EC system was positioned near the centre of the path, consisting of a sonic anemometer (R3, Gill Instruments, Lymington, UK) and open-path infrared gas analyser (IRGA) (LI-7500, LI-COR Biosciences, Lincoln, USA) mounted at 12.5 m above ground level (a.g.l.). The EC site was equipped with an automatic weather station (WXT 510/520, Vaisala, Finland) which provides the additional input data required to process the scintillometer data: temperature, relative humidity (RH), pressure (p) and wind speed (U) are measured at a height of 10.6 m. A four-component radiometer (NR01, Hukseflux, The Netherlands) was installed at 10.1 m on the same mast and a tipping bucket rain gauge (0.2 mm tip, Casella CEL, Bedford, UK) near the base of the mast. These were located in the garden of a residential property approximately 3 km north of the town centre, where the surrounding land use is predominantly residential, consisting of 1-2 storey houses with gardens. Full details are given in Ward et al. (2013a). In addition to the meteorological instrumentation at the EC site (MET_{sub}), a second weather station was established on the rooftop of a modern office building close to the town centre ($\mathrm{MET_{roof}}$). The setup is summarised in Table 1. To provide a combined dataset of continuous input variables required for scintillometry processing, T, RH, p and U from $\mathrm{MET_{roof}}$ were linearly adjusted to gap-fill $\mathrm{MET_{sub}}$ (required for < 1% of T, RH and p and < 2% of U data), based on regressions with concurrent data from $\mathrm{MET_{sub}}$ (9 May 2011 - 31 December 2012).

Northern Swindon is typical of suburban areas in the UK. The area has a relatively large proportion of vegetation and there is a large nature reserve just north of the centre of the study area, which lies directly underneath the scintillometer path. The town centre at the south of the study area has the highest density of buildings and roads (Figure 1). Industrial areas to the east and southwest with little vegetation contribute to measurement source areas under stable conditions (see Part 2). Despite the variety of land cover types, many neighbourhoods appear fairly homogeneous at a scale of a few hundred metres. The area shown in Figure 1 has land cover that is 14% buildings, 31% impervious, 53% vegetation, 1% water and 2% pervious. Land cover, topography and building and tree heights were derived from a spatial database for Swindon (5 m resolution, see Ward et al. (2013a) for more information).

Figure 1 Aerial photograph (2009, GeoPerspectives©) of the study area showing the locations of the two-wavelength scintillometer path (BLS-MWS), eddy covariance station (EC) and two meteorological stations (MET_{sub}, MET_{roof}). The location of Swindon within the British Isles is shown (top right).

Instrumentation	Height [m]	Location	Path length [m]	z_0 [m]	z_d [m]
Two-wavelength scintillometer system	44.3	51°36'33.9" N 1°47'38.6" W (Tx) 51°33'38.1" N 1°46'55.3" W (Rx)	5492	0.7	4.9
EC station	12.5	51°35'4.6" N 1°47'53.2" W	-	0.5	3.5
MET_{sub}	10.6 (WXT) 10.1 (NR01)	51°35'4.6" N 1°47'53.2" W	-	0.5	3.5
MET_{roof}	2.0 (WXT) 1.1 (NR01)	51°34'0.3" N 1°47'5.3" W	-	-	-

Table 1 The instrumental setup. For the scintillometers the mean height of the beam above the land surface (z_m) is given (for the effective measurement height (z_{ef}) see Table 2); for MET_{roof} the heights above the roof surface are given. Roughness length, z_0, and displacement height, z_d, were not calculated for the rooftop site. Tx denotes transmitter, Rx receiver.

To obtain representative measurements it is important to be high enough above the surface that quantities are sufficiently well-blended (i.e. high enough that turbulent mixing averages out the influence of surface heterogeneity), although recent studies have shown successful use of scintillometers even below the blending height (Meijninger et al. 2002b; Ezzahar et al. 2007). Based on the average height of the roughness elements (i.e. buildings and trees) the blending height is estimated at about 15-30 m for the BLS-MWS source area (Pasquill 1974; Garratt 1978). The scintillometer transmitters, mounted on custom-built brackets, were installed at 28 m a.g.l. on a television transmitter mast. The receivers of the BLS-MWS system were mounted at 26 m a.g.l. on a rooftop in Swindon town centre. The resulting path is slanted (Figure 2).

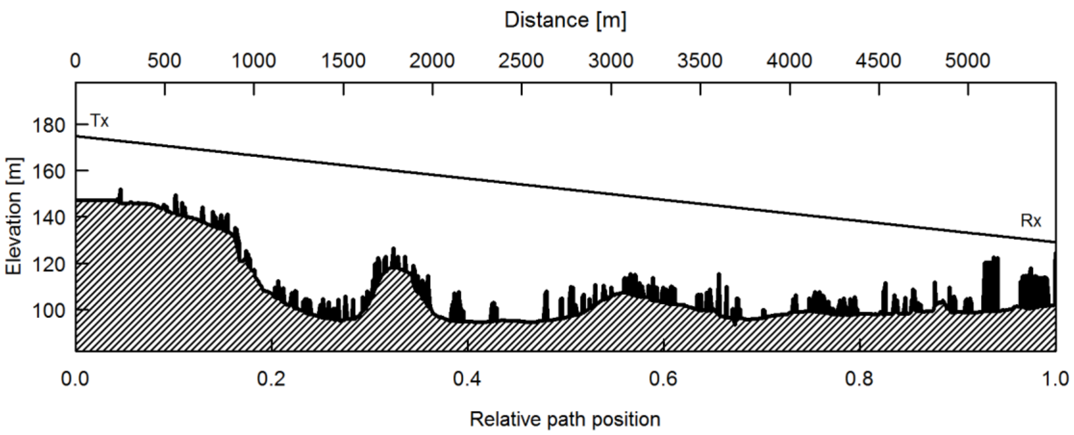

Figure 2 Cross-section of the land surface (metres above sea level) and height of obstacles (buildings and trees) along the BLS-MWS path. Tx denotes transmitter, Rx receiver.

The effective heights of the scintillometers are given in Table 2, calculated according to the stability-independent approximation (Equation 15 of Hartogensis et al. (2003)). These estimates include adjustment to account for the curvature of the earth and displacement height, z_d (Table 1). Displacement heights were calculated from the mean height of the roughness elements, z_H, within a distance of ±1000 m perpendicular to the scintillometer path (and +500 m in the direction parallel to the path), using the rule-of-thumb $z_d = 0.7z_H$ (Garratt 1992; Grimmond and Oke 1999). In the case of the EC station, z_H was calculated within 500 m of the EC mast. The difference in BLS and MWS path-weighting functions (Figure 3) means that the BLS, MWS and combined BLS-MWS covariance measurements are representative of different heights even though the BLS and MWS beams essentially traverse the same path (Evans and De Bruin 2011).

For the two-wavelength scintillometer system the BLS and MWS beams must be close together (Lüdi et al. 2005). The separation between beams was minimised (< 0.35 m) and the relative positions of the BLS and MWS were reversed at each end of the path so that the beams crossed near the centre of the path. It was necessary to shield cables at the scintillometer sites to protect against electrical interference. Scintillometer data can sometimes be affected by vibrations of the mounting structures (Von Randow et al. 2008; Beyrich et al. 2012). However, mounting brackets were designed with this in mind and the scintillometer spectra show little evidence of any vibrational contamination.

The data presented here are for the complete months when the BLS-MWS system was functioning: July-December 2011 and May-December 2012. From January 2012 to April 2012 the MWS was not operational due to a fault.

	Instrument characteristics		**Site-dependent characteristics**		
Scintillometer	**Wavelength [m]**	**Aperture diameter [m]**	**Fresnel zone [m]**	**Effective height [m]**	**Scaling (S) factor**
BLS (C_{n1n1})	880×10^{-9}	0.145	-	45.0	-
MWS (C_{n2n2})	3.2×10^{-3}	0.25	4	42.8	0.952
BLS-MWS (C_{n1n2})	-	-	-	43.1	0.958

Table 2 Instrument and site-dependent characteristics of the scintillometers and paired scintillometer system.

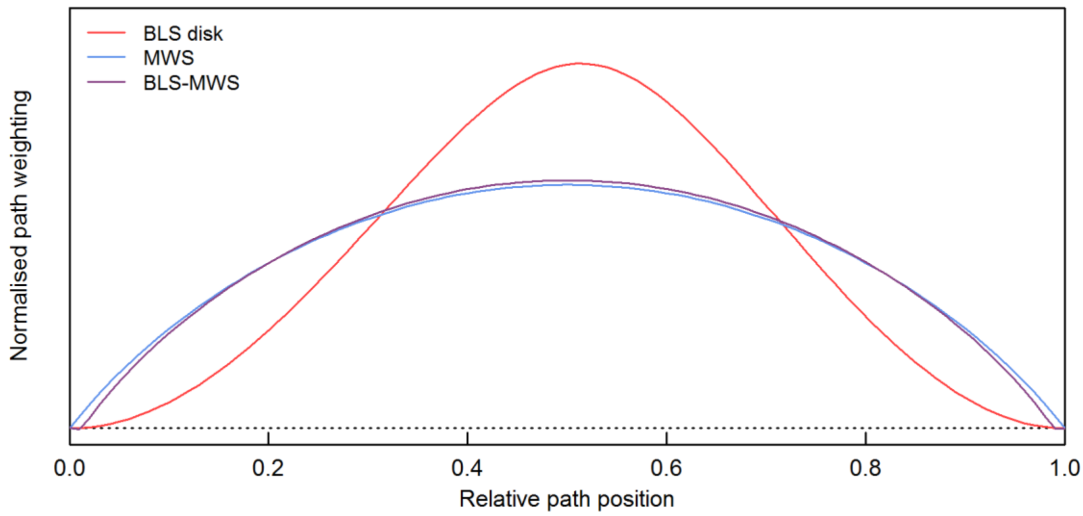

Figure 3 Path-weighting functions for the infrared scintillometer (BLS disk), the MWS and the BLS-MWS combination, normalised so that the total area under each curve equals one.

3.2. Data collection, processing and quality control

3.2.1. Scintillometry

In this study, C_{n1n1} is used to denote the refractive index structure parameter from the BLS, to distinguish from C_{n2n2} (MWS) and C_{n1n2} (BLS-MWS cross-term). The BLS900 is a dual-beam scintillometer with two transmitter disks (only one disk is used here for combination with the MWS). The signal intensity of each BLS disk was sampled and stored at 500 Hz (raw data) and statistics including the mean and standard deviation of signal intensity were provided at 30 s intervals by the Scintec software (SRun v1-07). Additionally, the signal intensities of both BLS disks and of the MWS were sampled at 100 Hz by a CR5000 datalogger (Campbell Scientific Ltd., Loughborough, UK). These data were processed using code written in R (The R Foundation for Statistical Computing). Data were subjected to initial quality control involving the removal of dropouts (when the BLS makes a background measurement) and despiking. The BLS and MWS signals were bandpass filtered to remove contributions below 0.06 Hz and above 20 Hz for the calculation of C_{n2n2} and C_{n1n2}. The low-frequency cut-off reduces the influence of absorption fluctuations. ~~At 10-min intervals the variances, covariances and mean values of the signals were calculated, from which the log-amplitude (co)variances (σ^2_χ) were obtained.~~ At 10-min intervals the variances, covariance and mean values of the signals were calculated, from which the log-amplitude variances ($\sigma^2_{\chi 1}$, $\sigma^2_{\chi 2}$) and covariance ($\sigma_{\chi 1 \chi 2}$) were obtained (Tatarski 1961). To convert between the log-amplitude (co)variances and refractive index (cross-)structure parameters the following equations were used:

$$C_{n1n1} = 4.48 D^{7/3} L^{-3} \sigma^2_{\chi 1}, \tag{14a}$$

$$C_{n2n2} = 8.33 k^{-7/6} L^{-11/6} \sigma^2_{\chi 2}, \tag{14b}$$

$$C_{n1n2} = 8.93 k^{-7/6} L^{-11/6} \sigma_{\chi 1 \chi 2}, \tag{14c}$$

where D refers to the aperture diameter of the infrared scintillometer, k to the wavenumber ($2\pi/\lambda$) of the millimetre-wave scintillometer and L to the path length (Table 1, Table 2). These equations can be derived from the full forms of the log-amplitude (co)variances, which express the path weighting of the instrument, aperture averaging by the finite size of transmitter and receiver, the turbulence spectrum (assumed to be the Kolmogorov spectrum, e.g. Monin and Yaglom (1971)) and separation of the beams if applicable (Equations A1, A2, Appendix A). Note that Equation 14c is specific to the setup described here (beam separation, path length and instrument characteristics) and could be expressed in terms of D rather than k. Equation 14b was obtained using the full formula (Equation A2) instead of the small aperture approximation (in which the Bessel functions accounting for aperture averaging are excluded) and is also specific to this setup. The approximation can result in an inaccuracy even for long paths (Appendix A). Equation 14a for the infrared scintillometer is a standard result and was first demonstrated by Wang et al. (1978).

Quality control procedures rejected data during periods of low signal strength (usually caused by rain or fog). BLS data were rejected when the received signal intensity dropped below 0.5 of the daily maximum value. For the MWS a threshold of 0.33 of the daily maximum intensity was used, and MWS data were also removed when the BLS signal intensity was below the 0.5 threshold indicating obscuration along the BLS-MWS path. The data points directly adjacent to those failing the signal strength checks were also removed. Rain was recorded at the EC site for 10% of the dataset and fog often occurred, particularly during autumn and winter mornings (based on observations during site visits). Values of C_n^2 ~~above~~ outside reasonable thresholds were excluded (nine C_{n1n1} values and one C_{n1n2} value). The resulting data available for analysis constitute 79% of the total possible 10-min values (N = 61776).

Kleissl et al. (2010) suggests an empirical threshold for the onset of saturation for infrared large aperture scintillometers of $C_{n1n1} > 0.074D^{5/3}\lambda^{1/3}L^{-8/3}$. Approximately 21% of the BLS data were above this threshold of 3.2×10^{-15} m$^{-2/3}$. BLS data were corrected for saturation using a look up table of numerical values based on the modulation transfer function of Clifford et al. (1974). The correction increased C_{n1n1} by around 5% overall (~10% during summer daytimes). Where the estimated correction was larger than 25% data were removed instead (46 values in total). MWS data were well below the saturation threshold of 5.0×10^{-11} m$^{-2/3}$ (Clifford et al. 1974) and were not corrected. The BLS-MWS covariance was not corrected as a methodology is yet to be determined (Beyrich et al. 2012). There is therefore increased uncertainty in these measurements due to the extent of currently applicable theory.

To use the refractive index structure parameters in Equation 6 (or Equation 10a-b), C_{n1n1}, C_{n2n2} and C_{n1n2} must be representative of the same height. The S factors (Evans and De Bruin 2011) given in Table 2 were applied to C_{n2n2} from the MWS and C_{n1n2} from the BLS-MWS to scale them to the same effective height as C_{n1n1} from the BLS. These factors account for the difference in effective heights between the three C_n^2 measurements resulting from the combination of different weighting functions and changing beam elevation along the path (Section 3.1). The S factors are relatively close to unity as the height differences are reasonably small for this setup. The approximation of using stability-independent S factors was made here (incorporating stability would give values ranging from 1.0 under very stable conditions to 0.9 for free convection). Calculation of the meteorological structure parameters proceeds as described in Section 2.

Data were processed using each of the three techniques in order to investigate their respective merits, although the focus is on the two-wavelength and bichromatic-correlation methods. No Bowen ratio correction was applied for the single-wavelength method (Equation 4), given the uncertainties in estimating the available energy in urban environments. The impact is estimated to be a 6% overestimation in C_T^2 (based on β from the two-wavelength method). The positions of twice-daily minima in C_{n1n1} were used to indicate stability transitions (Samain et al. 2012a) and assign positive or negative r_{Tq} for the two-wavelength method. For the two-wavelength method r_{Tq} = ±0.8 was assumed and the solution corresponding to $S_{2\lambda}$ = +1 was chosen. To distinguish between the methods applied (single-wavelength, two-wavelength, bichromatic-correlation), the subscripts '1λ', '2λ' and 'bc' are used.

3.2.2. Eddy covariance

Structure parameters were also derived from 20 Hz raw EC data. Sonic and IRGA data were time aligned by seeking maximum covariance between variables. Initial quality control incorporated threshold checks, outlier detection and despiking. A fixed temporal separation of τ = 1 s was decided upon after investigation into suitable values in the inertial subrange. Calculation of C_T^2, C_q^2 and C_{Tq} included the Schotanus et al. (1983) correction for sonic temperature as discussed in Braam (2008) and Braam et al. (2012). ~~No corrections for spectral losses were made, which can be expected to result in underestimations of about 5-7%.~~ No corrections were made for spectral losses due to the spatial separation of the sonic and IRGA and their finite path lengths, which can be expected to result in underestimations of about 5–7% (Hill 1991; Hartogensis et al. 2002).

The resulting 30-min structure parameters were quality controlled in accordance with the corresponding EC fluxes. Data were removed during times of known instrument malfunction, when the IRGA diagnostic indicated obstruction of the optical path, when rainfall could adversely affect the measurements and if values exceeded physically reasonable ranges.

To facilitate comparison between EC and scintillometer datasets, the EC structure parameters were scaled to match the height of the scintillometer data using MOST functions (with the constants suggested by Andreas (1988) and assuming identical height-scaling of temperature and humidity, see Equation 2a, b in Part 2).

Since the source areas are different between EC and BLS-MWS systems, the structure parameters obtained are not expected to be in perfect agreement. The BLS-MWS footprint is generally more vegetated than the EC footprint (56% versus 44%). However, comparisons are useful for a number of reasons. As EC is a widely-used technique, it permits evaluation of the scintillometer system to a certain extent, through comparison of trends and patterns of behaviour even if absolute values differ. Both systems have merits and limitations: scintillometers are spatially representative; EC is a more direct measurement but (open-path IRGAs) cannot provide data after rainfall and there are issues with energy closure (Foken 2008). Analysis of both approaches can therefore provide a more complete picture of the environment studied.

4. Instrument performance

An unidentified instrumental noise problem affecting the CEH-RAL MWS has been reported elsewhere (Van Kesteren 2008; Evans 2009; Beyrich et al. 2012). Following extensive testing, the cause of the issue was finally established and the instrument repaired in June 2011. The spectra obtained are now close to the ideal shapes predicted by theory and suggest good instrument performance with a low noise floor (Figure 4). An upper estimate for the MWS noise limit is $C_{n2n2} \sim 1 \times 10^{-15}$ m$^{-2/3}$. The observed noise limit of the BLS is of the order of $C_{n1n1} \sim 5 \times 10^{-17}$ m$^{-2/3}$ in agreement with the manufacturer's specification (Scintec 2009).

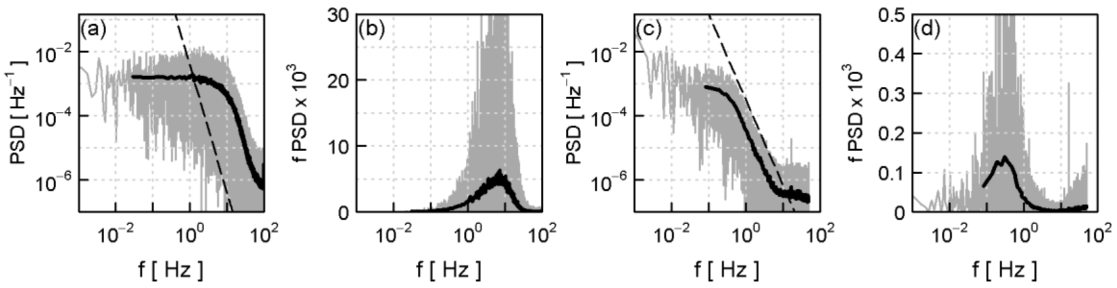

Figure 4 Example power spectral density (PSD) and frequency (*f*) spectra for (a, b) the BLS and (c, d) unfiltered MWS for 14:30-15:00 UTC on 02 July 2011. Smoothed spectra (data divided into 100 bins) are shown in black. The dashed lines represent theoretically predicted slopes of -12/3 and -8/3 for the BLS and MWS respectively.

5. Results and discussion

5.1. Structure parameters

5.1.1. Refractive index structure parameters

The refractive index structure parameters measured by the BLS (C_{n1n1}) and MWS (C_{n2n2}) and the cross-structure parameter from the covariance of the BLS-MWS signals (C_{n1n2}) follow clear diurnal cycles. Data for an example day are plotted in Figure 5. Whilst C_{n1n1} and C_{n2n2} remain positive, the cross-structure parameter can be positive or negative depending on whether the infrared and millimetre-wave signals are correlated or anti-correlated. C_{n1n2} tends to be negative during the day and positive at night. The sign change occurs at the morning and evening stability transitions. Typically C_{n1n1} passes through sharp minima at these times, whereas the diurnal course of C_{n2n2} is flatter and wider, without clearly defined minima. These findings are in broad agreement with data from the LITFASS campaigns (Beyrich et al. 2005; Lüdi et al. 2005; Beyrich et al. 2012).

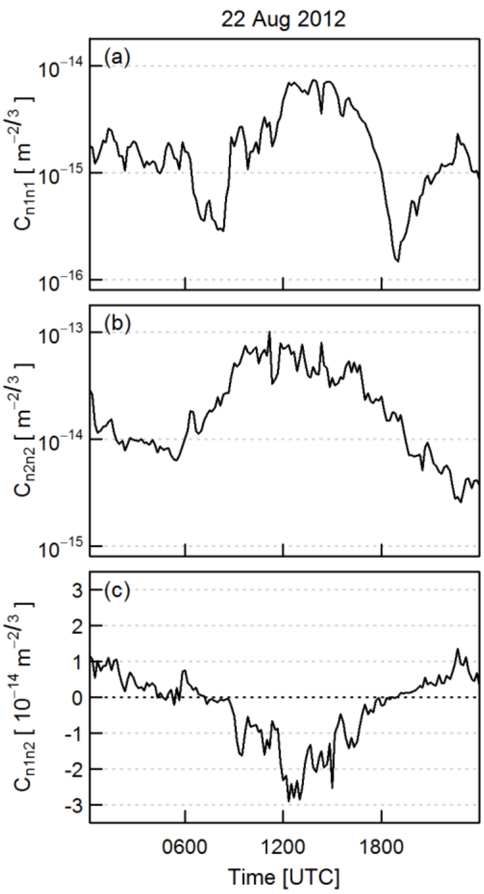

Figure 5 Structure parameters of the refractive index as measured by (a) the BLS and (b) the MWS, and (c) the cross-structure parameter as measured by the BLS-MWS combination for an example day (22 August 2012).

When averaged by month (Figure 6), the diurnal patterns are enhanced and seasonal trends are revealed. The amplitudes of the diurnal cycles are largest in summer, except C_{n1n1} which peaks slightly earlier in the year. C_{n1n1} is closely related to C_T^2 and, in turn, the sensible heat flux. Hence the peak in C_{n1n1} in late spring reflects the annual cycle of Q_H: approaching maximum insolation in mid-summer, the total energy input is large but evapotranspiration rates are limited by phenological development as maximal leaf area is not reached until later in the year. During winter, low radiative input means the midday maximum in C_{n1n1} is small; larger values are observed at night. For millimetre wavelengths C_{n2n2} tends to remain low throughout the night. The diurnal cycle in C_{n1n2} is maintained across all months with changes in the position of the zero-crossings determined mainly by atmospheric stability (usually the sign of Q_H, related to available energy and day length). In

December C_{n1n2} is negative only for a very short period during the middle of the day. The effect of day length is also seen in the positions of C_{n1n1} minima, which move closer together as radiative energy input decreases from summer to winter. Using the positions of C_{n1n1} minima to indicate the stability transition times generally worked well for this dataset, although performance was poorer in winter when stability changes tend to be less well defined and conditions may remain close to neutral throughout the day. Following the method described in Samain et al. (2012a), additional restrictions were imposed on the times of morning (here after 0400 UTC) and evening (before 2100 UTC) transitions. In a few cases, cumulative daily net radiation was also used to distinguish C_{n1n1} minima that were due to sudden cloud cover during daytime from C_{n1n1} minima that were due to a change of stability.

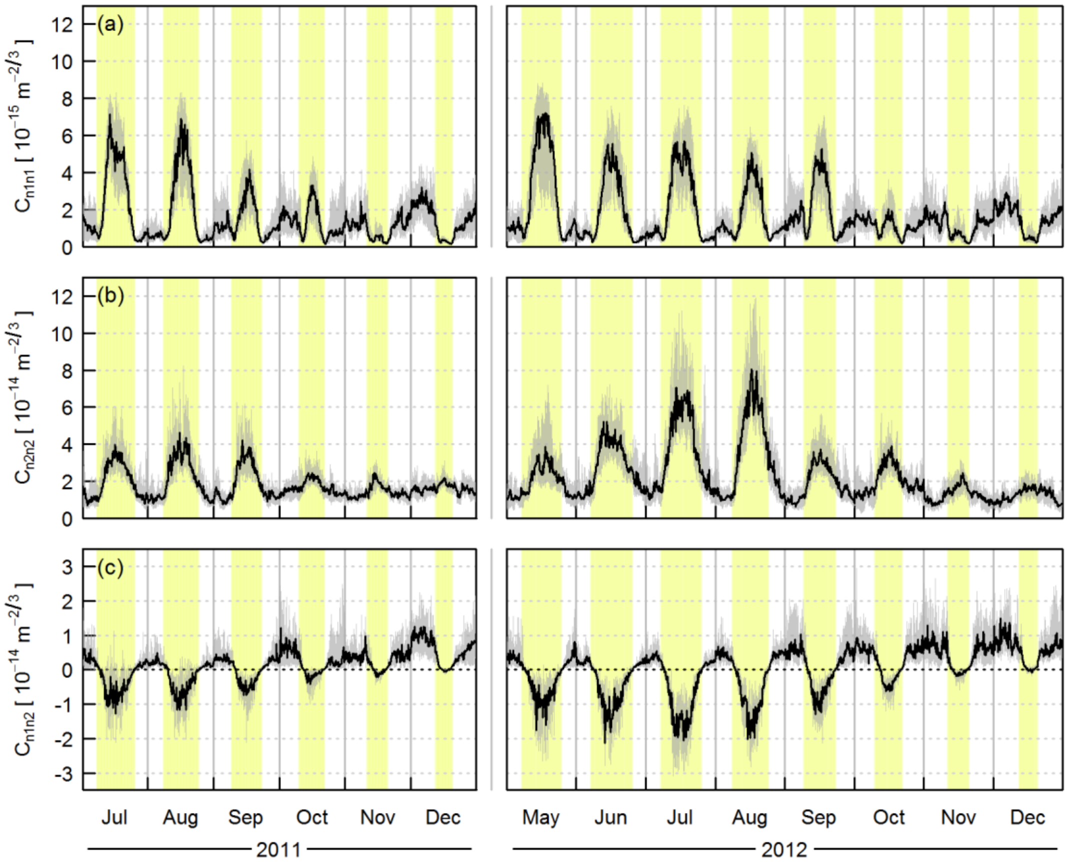

Figure 6 Median diurnal cycles and inter-quartile ranges (shading) of the structure parameters of the refractive index as measured by (a) the BLS and (b) the MWS, and (c) the cross-structure parameter as measured by the BLS-MWS combination, separated by month. Yellow shading indicates periods when $Q^* > 0$ W m^{-2}.

5.1.2. Meteorological structure parameters

There are clear parallels between the refractive index structure parameters (Figure 6) and the meteorological structure parameters (Figure 7). C_{n1n1} is dominated by C_T^2 with a small contribution from C_{Tq} (of about 5%, which decreases as β increases (Green et al. 2001)). The cross-structure parameter C_{n1n2} consists mostly of the C_{Tq} term and a contribution from C_T^2. When C_{n1n2} is negative C_{Tq} is positive. The dominant term in C_{n2n2} depends on the Bowen ratio: C_q^2 usually dominates at low β but the C_{Tq} term is important too and forms a negative contribution to C_{n2n2} during daytime (when C_{Tq} is positive).

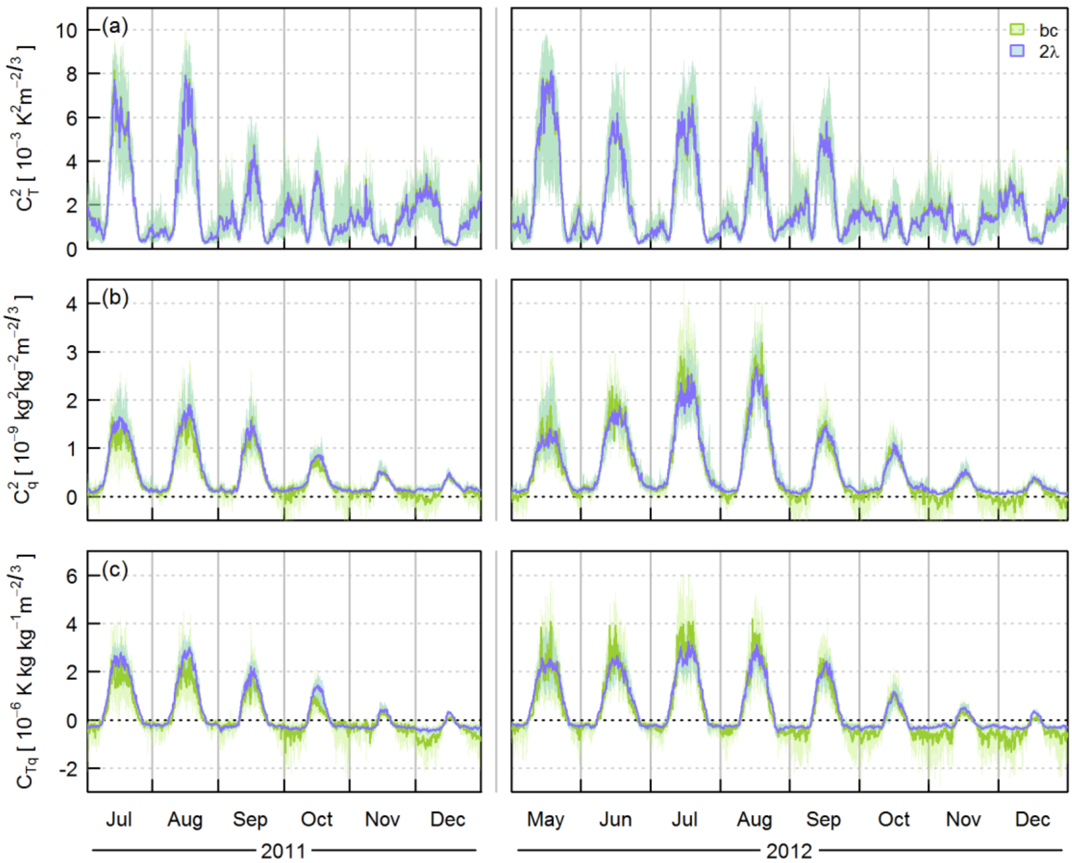

Figure 7 Median diurnal cycles and inter-quartile ranges (shading) of the meteorological structure parameters (a) C_T^2, (b) C_q^2 and (c) C_{Tq} calculated using the bichromatic (bc) and two-wavelength (2λ) techniques. In (c) C_{Tq} for the two-wavelength technique is given by ±0.8$(C_T^2 C_q^2)^{1/2}$.

5.1.3. Comparison of eddy covariance and scintillometry techniques

In Figure 8, meteorological structure parameters for individual days are compared to EC. As structure parameters are strongly height dependent, the EC values have been scaled to match the height of the scintillometry results (z_{ef} = 45.0 m, Section 3.2.2). Scintillometer and EC values of C_T^2 and C_q^2 are not expected to agree exactly due to the differences in source area and land cover composition, however, these independent measurements are often remarkably consistent. The correlation between the scintillometer and EC datasets gives confidence that the scintillometer setup is responding reasonably to changes in boundary layer conditions and measuring within the surface layer. The square of the correlation coefficient (r^2) between the two-wavelength scintillometry and height-scaled EC data is 0.72 and 0.60 for C_T^2 and C_q^2 respectively. Considering daytime only, r^2 increases to 0.86 for C_T^2, but remains about the same for C_q^2 at 0.56.

~~Height-scaled $C_{T\_EC}^2$ closely matches $C_{T\_BLS\text{-}MWS}^2$, with values being more similar during the day than the night. On the other hand, height-scaled $C_{q\_EC}^2$ is much smaller than $C_{q\_BLS\text{-}MWS}^2$, with closer agreement before height-scaling.~~ These results suggest $\beta_{\_EC}$ is larger than $\beta_{\_BLS\text{-}MWS}$, but the fact that the estimates of C_T^2 are closely matched while $C_{q\_BLS\text{-}MWS}^2$ is larger than $C_{q\_EC}^2$ is indicative of a more complex situation (see Part 2).

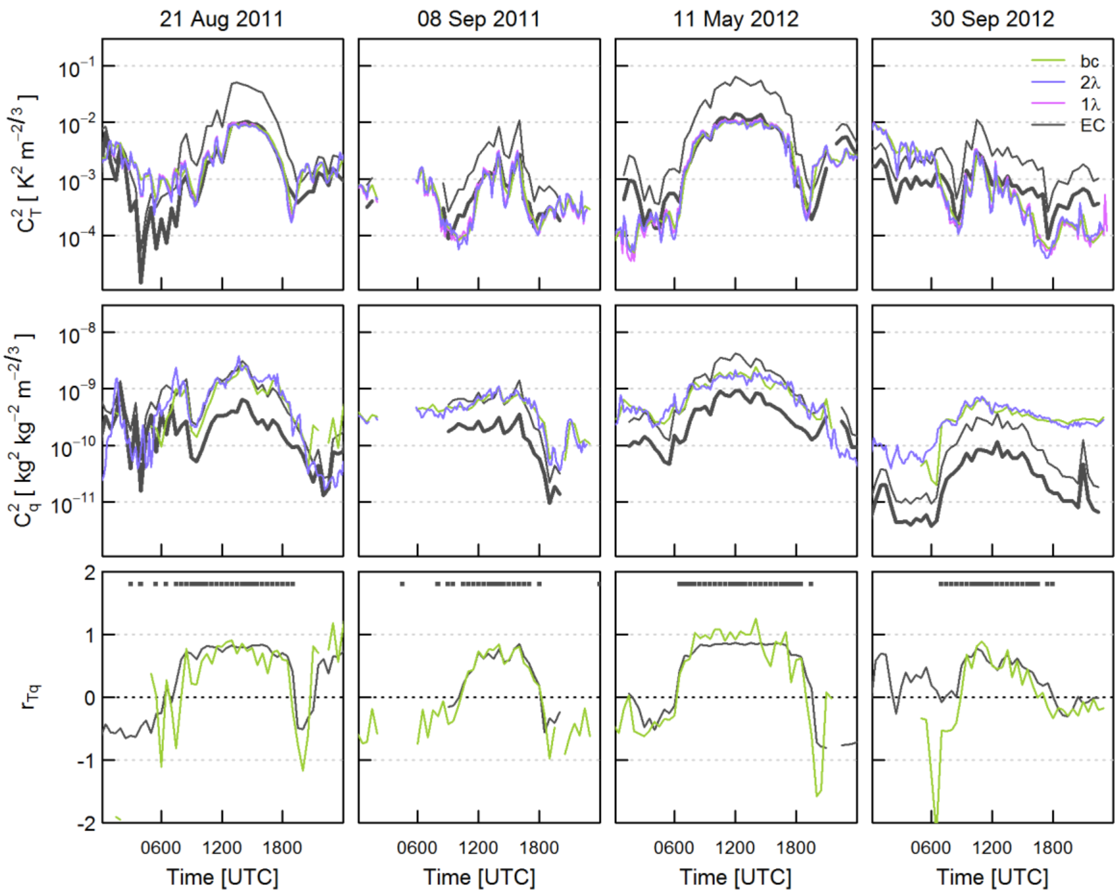

Figure 8 Structure parameters of temperature and humidity and the temperature-humidity correlation coefficient for selected days, derived from eddy covariance measurements (EC) and from the BLS-MWS system using the single-wavelength (1λ), two-wavelength (2λ) and bichromatic-correlation (bc) methods. EC structure parameters are shown for the EC measurement height (thin line) and scaled to the effective height of the scintillometry results (thick line). Unstable times according to the EC data (L_{Ob} < 0) are indicated by grey dots. Single-wavelength and two-wavelength data are for 10-min intervals; EC and bichromatic-correlation data are for 30-min intervals.

Structure parameters from the BLS-MWS and EC systems exhibit the same trends (but have different magnitudes) over the course of the year (Figure 9). C_T^2 is largest during late spring, whilst C_q^2 peaks in July and August. There is variability between years attributed to drier conditions in 2011 than 2012 (July-August rainfall was 110 mm in 2011, 184 mm in 2012). In July-August 2011, C_T^2 was larger and C_q^2 smaller than in the same months in 2012. In general, 2012 was much wetter than 2011 which explains consistently lower β in 2012 (Figure 9c). The BLS-MWS gives lower β compared to EC (during summer daytime $\beta_{BLS\text{-}MWS}$ ≈ 0.5 and β_{EC} ≈ 1.0), which is in accordance with the BLS-

MWS footprint being more vegetated, but similar seasonal behaviour is seen. In winter β becomes negative as a result of reduced radiative input, and the difference between $\beta_{BLS-MWS}$ and β_{EC} decreases. In terms of ~~energy exchange~~fluxes, evapotranspiration continues throughout winter because ~~the availability of~~ moisture is readily available, ~~means evaporation continues throughout winter~~ whereas energy is limited so Q_H is directed towards the surface for much of the daytime, only becoming positive for a short time around midday ~~when there is sufficient energy~~ (Ward et al. 2013a). Although it is more straightforward to consider this behaviour in terms of the fluxes (discussed further in Part 2), the same conclusions could be inferred from the diurnal course of r_{Tq} (Figure 10) and positions of C_{n1n1} minima (Figure 6a).

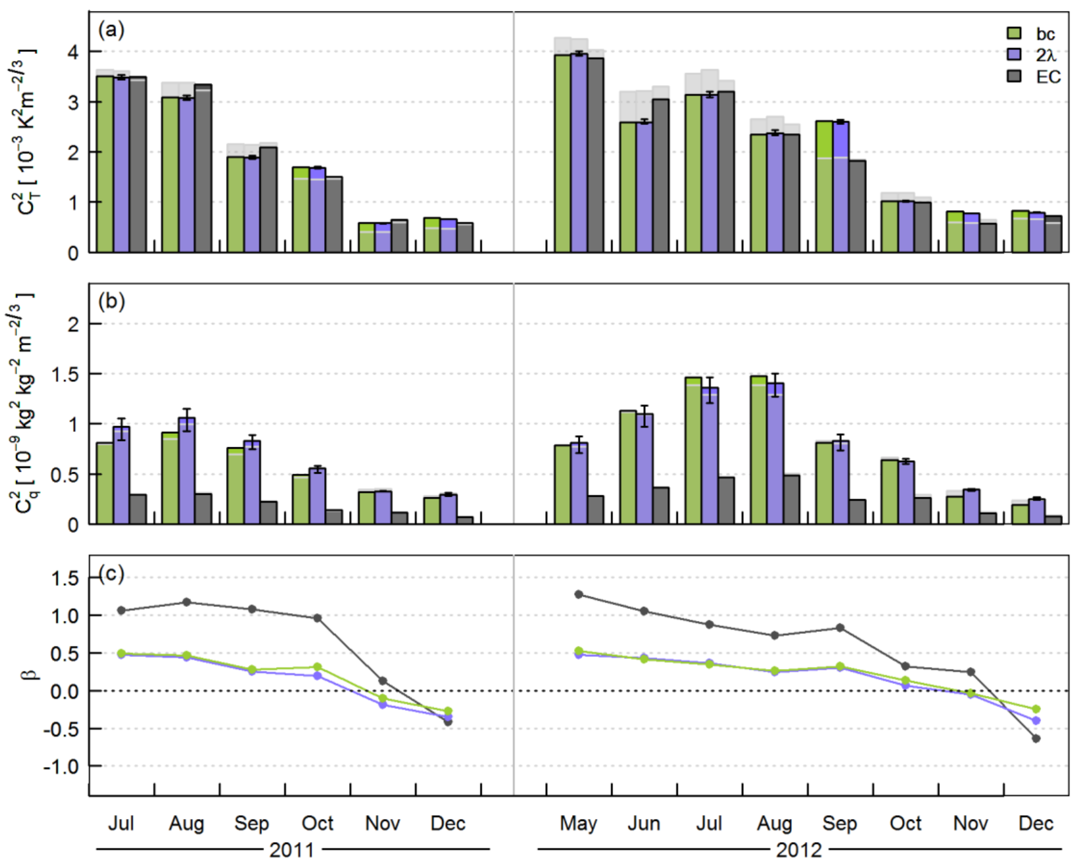

Figure 9 Mean daytime (incoming shortwave radiation $K_{\downarrow}$ > 5 W m^{-2}) (a-b) structure parameters ~~(a-b)~~ and (c) Bowen ratio ~~(c)~~calculated according to Equation 9 for each month calculated for the BLS-MWS system (bichromatic-correlation and two-wavelength approaches) and eddy covariance data scaled to match the BLS-MWS height. For the two-wavelength

results $r_{Tq\_2\lambda}$ = ±0.8; error bars in (a) and (b) indicate the effect of assuming r_{Tq} values of ±0.5 and ±1.0. Light grey bars (a, b) indicate means calculated when both C_T^2 and C_q^2 from all three methods (bc, 2λ and EC) are available.

The performance of EC and scintillometry differs with atmospheric conditions. EC data from open-path gas analysers cannot be used if the instrument windows are wet, such as during and after rainfall (Heusinkveld et al. 2008). Consequently, water vapour measurements from open-path systems significantly under-represent these times and may result in an appreciable underestimation of mean Q_E (Ramamurthy and Bou-Zeid 2014) and C_q^2. Mean values for C_T^2 calculated using daytime data only when all quantities are available concurrently (i.e. C_T^2 and C_q^2 from EC, two-wavelength and bichromatic-correlation methods (grey bars, Figure 9)) are larger compared to mean values calculated using all available daytime data (coloured bars) due to the exclusion of periods during and directly following rain (when C_T^2 is typically relatively low Q_E is relatively high). In September 2012 the opposite effect is seen because the EC data were limited by dirty IRGA windows when the weather was dry and sunny, hence it is generally high C_T^2 values that are eliminated in this case. During summer, monthly mean $C_{q\_BLS\text{-}MWS}^2$ is reduced slightly for the concurrent dataset (grey bars) as times of high Q_E when water and energy are plentiful have been excluded. The overall results are not substantially changed for the restricted subset: $C_{T\_BLS\text{-}MWS}^2$ and $C_{T\_EC}^2$ are still similar whilst $C_{q\_BLS\text{-}MWS}^2$ still exceeds $C_{q\_EC}^2$, although the difference between $C_{q\_BLS\text{-}MWS}^2$ and $C_{q\_EC}^2$ is reduced slightly. The spectral correction (Section 3.2.2) would increase the EC structure parameters by 5-7%, which would further reduce the discrepancy between EC and BLS-MWS values.

As for most previous two-wavelength campaigns, typical Bowen ratios for this path are expected to lie below the problematic region of minimum C_{n2n2} (Section 2.1). Other urban studies suggest daytime β of around 1.0-1.5 for suburban sites, lower when precipitation is frequent (Grimmond and Oke 1995) and strongly dependent on the amount of vegetation (Grimmond and Oke 2002; Christen and Vogt 2004). However, although average β remains below 1.5 (Figure 9c), changing surface conditions can drive down the evapotranspiration on the timescale of a few days (e.g. drying of impervious surfaces (Ward et al. 2013a) or, at agricultural sites, senescing crops (Evans et al. 2012)), producing substantial excursions from the average β. Such excursions are seen in this dataset, particularly for β_{EC}, whereas $\beta_{2\lambda}$ seems to be limited to values ≤ 1.3. There are two potential issues here: (a) the two-wavelength sign ambiguity and (b) the region of reduced sensitivity around the C_{n2n2} minimum (Section 2.1). Selecting $S_{2\lambda}$ = +1 automatically restricts $\beta_{2\lambda}$ to values below that at which the terms in Equation 3 cancel out ($\beta_{2\lambda\_min}$ = 2.0-2.6 for this dataset). For a few cases (when β is large), the 'true' structure parameters should be obtained from the alternative solution ($S_{2\lambda}$ = -1). Using the bichromatic-correlation results to identify times of high β suggests the impact is small (β_{bc} > $\beta_{2\lambda\_min}$ for a very small proportion of the data (< 0.3% of daytime values)). A more significant issue appears to be reduced measurement capability for $\beta_{2\lambda}$ > 1.3. As the true β increases, if C_{n2n2} does not decrease as much as expected from theory, $\beta_{2\lambda}$ will likely be underestimated, and the corresponding C_q^2 (and Q_E) could be overestimated. It is thought that noise in the setup (instrumental or unwanted intensity fluctuations from absorption, for example) may constrain the measured value of $\beta_{2\lambda}$ to a greater extent than suggested in the literature.

This region of reduced sensitivity of C_{n2n2} also compromises the performance of the bichromatic method, as measured C_{n2n2} will be mostly made up of noise contributions relative to the near-zero true value of C_{n2n2}. It follows that the correlation between BLS and MWS signals in this region is expected to be dominated by common instrumental or atmospheric effects such as absorption, or any electrical interference, mounting vibrations or obscuration along the path. Although these effects were not found to be problematic generally, they could become significant when the refraction signal diminishes at moderate β.

5.1.4. Comparison of two-wavelength and bichromatic-correlation methods

The three estimates of C_T^2 for the BLS-MWS path are similar (on average within 6%) whether the bichromatic-correlation, two-wavelength or single-wavelength approach is used. Larger deviations are seen between $C_{q\_bc}^2$ and $C_{q\_2\lambda}^2$ when measured r_{Tq_bc} differs from the value assumed (±0.8) in the two-wavelength method (e.g. 21 August 2011, Figure 8). During daytime, $C_{q\_2\lambda}^2$ is slightly larger than

$C_{q\_bc}^2$ in 2011 but the opposite is true for most of 2012 (Figure 7b, Figure 9b). This could be due to higher values of r_{Tq_bc} in 2012 (see Figure 10), which result in smaller C_T^2 but larger C_q^2 when $r_{Tq} > 0$. The value of r_{Tq} has a greater impact on C_q^2 than C_T^2 (compare error bars in Figure 9a, b). Had $r_{Tq\_2\lambda}$ been assumed to be ±1.0 instead of ±0.8, $C_{q\_2\lambda}^2$ would have been 7% higher and $C_{T\_2\lambda}^2$ 1% lower.

During winter night-times, large differences are observed between $C_{q\_bc}^2$ and $C_{q\_2\lambda}^2$ which cannot be explained by differences in r_{Tq}. Negative values of $C_{q\_bc}^2$ are frequently obtained (Figure 7b). These do not have a physical interpretation but are indicative of measurement limitations and coincide with large negative C_{Tq_bc}, which results from large positive C_{n1n2} (i.e. high correlation between BLS and MWS beams). Particularly during these times, but also in general, the bichromatic-correlation data show much greater variability than the two-wavelength data. To reduce this variability, bichromatic-correlation data are presented as 30-min averages, other than in Figure 7.

~~As for most of the previous two-wavelength campaigns, typical Bowen ratios for this path are expected to lie below the problematic region of minimum C_{n2n2} (Section 2.1). Other urban studies suggest daytime β of around 1.0-1.5 for suburban sites, lower when precipitation is frequent (Grimmond and Oke 1995) and strongly dependent on the amount of vegetation (Grimmond and Oke 2002; Christen and Vogt 2004). However, although average β remains below 1.5 (Figure 9c), changing surface conditions can drive down the evaporation on the timescale of a few days (e.g. drying of impervious surfaces (Ward et al. 2013a) or, at agricultural sites, senescing crops (Evans et al. 2012)), producing substantial excursions from the average β. Such excursions are seen in this dataset, particularly for β_{EC}, whereas $\beta_{2\lambda}$ seems to be limited to values ≤ 1.3. There are two potential issues here: (a) the two-wavelength sign ambiguity and (b) the region of reduced sensitivity around the C_{n2n2} minimum (Section 2.1). Selecting $S_{2\lambda} = +1$ automatically restricts $\beta_{2\lambda}$ to values below that at which the terms in Equation 3 cancel out ($\beta_{2\lambda\_min} = 2.0$-$2.6$ for this dataset). For a few cases (when β is large), the true structure parameters should be obtained from the alternative solution ($S_{2\lambda} = -1$). Using the bichromatic-correlation results to identify times of high β suggests the impact is small (β_{bc}~~

~~> $\beta_{2\lambda\_min}$ for a very small proportion of the data (< 0.3% of daytime values)). A more significant issue appears to be reduced measurement capability for $\beta_{2\lambda}$ > 1.3. As the true β increases, if C_{n2n2} does not decrease as much as expected from theory $\beta_{2\lambda}$ will likely be underestimated, and the corresponding $C_q^{\ 2}$ (and Q_E) could be overestimated. It is thought that noise in the setup (instrumental or unwanted intensity fluctuations from absorption, for example) may constrain the measured value of $\beta_{2\lambda}$ to a greater extent than suggested in the literature.~~

~~The region of reduced sensitivity of C_{n2n2} also compromises the performance of the bichromatic method, as measured C_{n2n2} will be mostly made up of noise contributions relative to the near-zero true value of C_{n2n2}. It follows that the correlation between BLS and MWS signals in this region is expected to be dominated by common instrumental or atmospheric effects such as absorption, or any electrical interference, mounting vibrations or obscuration along the path. Although these effects were not found to be problematic generally, they could become significant when the refraction signal diminishes at moderate β.~~

5.2. Temperature-humidity correlation

Measured r_{Tq_bc} follows similar seasonal and diurnal trends to r_{Tq_EC} (Figure 10). During summer, there is a clear plateau of ~~close to +1~~around 0.8 during daytime and the transition times when r_{Tq} changes sign are of short duration compared to the day length. In winter r_{Tq} remains below zero for most of the day but peaks at positive values around midday, though the average midday r_{Tq} is less than 1. The EC data rarely exceed the range -0.75 to 0.85, whereas inspection of the time-series reveals that r_{Tq_bc} almost always follows a typical diurnal course but individual points may vary about the general trend (e.g. Figure 8). Some unrealistic values of $|r_{Tq\_bc}|$ > 1 are observed, even when averaged to 30 min (Figure 8; Figure 10). Lüdi et al. (2005) also reported frequent occurrences of $|r_{Tq\_bc}|$ > 1. Since r_{Tq} is a correlation coefficient these values (> 1) do not have a physical interpretation, but result from uncertainties and thus indicate limitations of the measurement. The uncertainty in C_{n1n2} is around 20% at best (Lüdi et al. 2005). This inherent uncertainty associated with individual measurements means the structure parameters from the bichromatic-correlation method show greater variability than from the two-wavelength method (Section 5.1.4), particularly C_q^2 and C_{Tq} which have a greater dependence on C_{n1n2} than C_T^2 does. For this reason, bichromatic results are presented at 30 min, rather than 10 min as for the two-wavelength method (Figure 8-Figure 11). In addition, to calculate r_{Tq}, the structure parameters must be combined (Equation 8) and so r_{Tq} amasses the uncertainties in each of the measurements.

Despite the high uncertainty, average r_{Tq} values provide information on the typical temperature-humidity correlation along the scintillometer path. This is an important quantity in its own right, as well as an indication of MOST violations. The literature suggests r_{Tq} is typically expected to be slightly less than +1 during the day, but negative and of smaller magnitude at night (Kohsiek 1982; Andreas et al. 1998; Meijninger et al. 2002a; Beyrich et al. 2005). According to Lüdi et al. (2005) the T-q anti-correlation observed at night is 'less pronounced' than the positive correlation during daytime; Meijninger et al. (2006) also found r_{Tq} ranged between -0.5 and 0.9. Our measurements conducted in the suburban environment do not indicate lower T-q correlation than over other surfaces. Indeed, it is thought that r_{Tq_EC} likely underestimates the true values (as the sonic and IRGA are spatially separated). This supports the use of MOST and gives confidence that the measurements are made at sufficient height that the effects of surface heterogeneity are well-blended. Furthermore, the two-wavelength assumption r_{Tq} = +0.8 is seen to be reasonable for unstable conditions, although probably r_{Tq} = -0.8 is too large during stable conditions. Figure 10 suggests that these assumptions are less justified in winter.

In Figure 11 values of r_{Tq} measured in this study are separated into unstable and stable conditions (based on L_{Ob} from EC data and the timing of stability transitions according to C_{n1n1} for the scintillometer data). During unstable conditions, measured r_{Tq} is positive and around 0.6 to 0.9 whereas the stable values tend to be smaller at around -0.3 to -0.5 and more variable. In winter r_{Tq} is smaller and more variable (median r_{Tq_EC} decreases from > 0.7 in summer to < 0.5 in December for unstable conditions). Some studies have indicated a dependence of temperature-humidity correlation on L_{Ob}, with larger deviations from MOST as neutral conditions are approached (Li et al. 2011; Nordbo et al. 2013), although other studies differ (De Bruin et al. 1993; Roth 1993). Part 2 further explores the scaling of temperature and humidity structure parameters with stability.

Some instances of positive nocturnal r_{Tq} are observed when the fluxes have the same signs – i.e. either unstable (Q_H > 0) conditions prevail, or more frequently observed is dewfall (Q_E < 0) under stable conditions (as on 21 August 2011 after 2130, Figure 8). In these cases the two-wavelength method is limited as negative r_{Tq} must be assumed in the absence of other information, whereas the bichromatic-correlation method often captures this behaviour. In general, nocturnal structure parameters (and fluxes) tend to be small so the absolute errors introduced by $r_{Tq\_2\lambda}$ of the wrong sign are fairly small, though they will always be biased in the same direction and so will accumulate over time.

The bichromatic-correlation data suggest larger daytime r_{Tq} in 2012 compared to 2011 but this is not seen in the EC data. The contrast between patches of hot, dry impervious areas and cool, wet vegetation may be reduced by altogether wetter surfaces in 2012, which is thought to increase correlation between temperature and humidity (Lamaud and Irvine 2006; Moene and Schüttemeyer 2008; Ramamurthy and Bou-Zeid 2014). On the other hand, Lüdi et al. (2005) found lower r_{Tq} coincides with lower β. Experiments designed to investigate the behaviour of r_{Tq} (and the performance of the bichromatic-correlation technique) under different conditions would be beneficial.

In winter, and also during night-time, turbulence tends to be less well-developed. This presents challenges to measurement theory. Measurements are also more likely to be outside the surface layer when stable stratification occurs and the boundary layer height is smaller. Due to the rough surface, near neutral conditions were far more common than stable and, for the most part, there remains a close match between the diurnal behaviour of EC and scintillometer measurements. On the few occasions when strongly stable conditions were observed at the EC station, comparison of time-series indicated periods when the BLS-MWS was ~~likely higher in the atmospheric boundary layer than is ideal~~possibly above the surface layer, and thus potentially affected by other processes not related to surface fluxes. However, these were relatively rare occurrences.

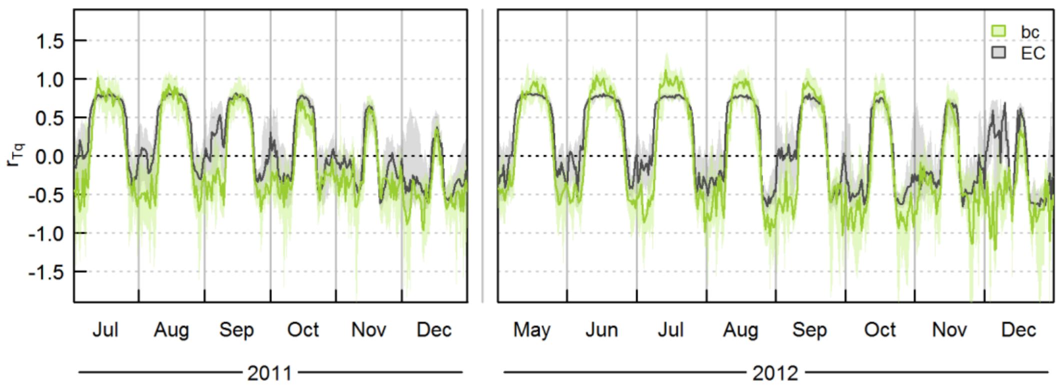

Figure 10 Monthly median diurnal cycles and inter-quartile ranges (shading) of the temperature-humidity correlation coefficient calculated from the BLS-MWS system via the bichromatic-correlation method and from EC.

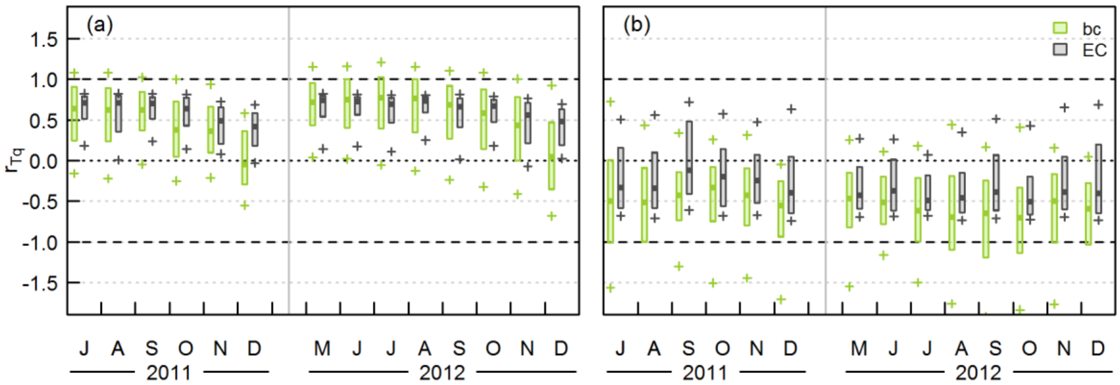

Figure 11 Boxplots of r_{Tq} from eddy covariance (EC) and the BLS-MWS bichromatic-correlation method for (a) unstable and (b) stable conditions. Crosses indicate the 10^{th} and 90^{th} percentiles, boxes enclose the inter-quartile range (25^{th} to 75^{th} percentiles) and heavy lines indicate the medians.

In this study, the performance of the bichromatic-correlation method was generally observed to be poor under conditions of low crosswind speeds (the wind speed component perpendicular to the BLS-MWS path). At times of low or near-zero crosswinds (< 2 m s^{-1}), the retrieved ~~values~~ quantities are less robust, $|r_{Tq\_bc}| > 1$ is commonly observed and r_{Tq_bc} is highly variable frequently changing sign (even during the day when both turbulent fluxes are reasonably expected to be positive and EC data do not suggest otherwise). The reason for this is unknown, but two possible explanations are considered here. Firstly, Taylor's frozen turbulence hypothesis is assumed in order to relate intensity fluctuations to C_n^2 (Clifford 1971; Wang et al. 1981). When crosswind speeds are low, this assumption is less justified and eddies decay as they are slowly blown through the beam. Correlation between the received scintillation pattern from one sample to the next is reduced compared to higher crosswind cases (Poggio et al. 2000). Correlation between the scintillation signals of the BLS and MWS will likely show greater variation too, depending on how the decay of eddies affects each beam, which would result in variability in C_{n1n2} that propagates through to r_{Tq_bc}. Secondly, when wind speeds are low, turbulence may be sporadic and not well-developed over the whole path length. Perhaps sudden gusts or turbulence events cause spuriously high correlation between BLS and MWS signals which outweighs the correlated scintillation signal the technique aims to measure. Given the complexity of this suburban site it is difficult to draw firm conclusions on this apparent effect of crosswind on bichromatic scintillometry at this stage. Given that the position of the spectrum is known to change with wind speed (Medeiros Filho et al. 1983; Nieveen et al. 1998; Ward et al. 2011), and that C_n^2 can be underestimated if the filter excludes part of the scintillation signal under very low wind speed conditions (Solignac et al. 2012), the suitability of the bandpass filter was also re-examined. However, the choice of filter frequency did not seem to explain the poor performance and modifying the filter frequencies did not resolve the issues. Small changes in filter frequency generally did not produce substantial changes to the results, suggesting that the frequencies chosen are suitable for this dataset, but it is not critical that those exact values are used.

6. Conclusions

This study reports the first use of a two-wavelength scintillometer system in an urban area. The behaviour of structure parameters and temperature-humidity correlation is investigated at various timescales. By examining the structure parameters themselves, more direct insight into the performance of the measurement techniques is gained; assessment of fluxes introduces additional uncertainties (e.g. similarity functions). Furthermore, structure parameters are important quantities in their own right. The spatial and temporal resolution of scintillometry observations offers advantages for assimilation into or evaluation of hydro-meteorological models. One approach for achieving this would be to work with structure parameters directly, rather than fluxes (e.g. Wood et al. 2013).

The structure parameters presented here extend previous observations to a different climatic region, different land cover type and, most importantly, across a much longer time period. Summertime behaviour is broadly in agreement with other published trials (Beyrich et al. 2005; Lüdi et al. 2005) but the long time-series presented here offers insight into seasonal variations. Day length, or more specifically, atmospheric stability, has a distinctive impact on the diurnal cycle of structure parameters and r_{Tq}. Overall, the structure parameters obtained from the BLS-MWS and EC systems exhibit remarkably similar tendencies. The Bowen ratio calculated from the measured structure parameters decreases across the two summer-to-winter periods studied here and $\beta_{BLS\text{-}MWS}$ is smaller than β_{EC}, attributed partly to different source area characteristics but also probable differences between the observational techniques. Part 2 explores energy partitioning further via turbulent fluxes.

As well as extending the two-wavelength technique to a new environment, several recently developed improvements have been implemented in the processing. To obtain the structure parameter of refractive index from the millimetre-wave scintillometer, the validity of the small aperture approximation is considered ~~(Appendix A)~~ and the more accurate full formula used instead ~~(Equation 14b, for this setup)~~. To adjust for the difference in effective heights between the BLS and MWS, the S factor approach of Evans and De Bruin (2011) was used. The structure parameters use the specific humidity formulation outlined in Ward et al. (2013b). The cross-correlation between BLS and MWS signals enabled estimation of the temperature-humidity correlation coefficient, thus extending the application of the bichromatic-correlation method to the suburban surface.

The bichromatic-correlation method sometimes returns values outside the physically meaningful range $|r_{Tq}| \leq 1$. The inherent variability of the cross-structure parameter C_{n1n2} limits the accuracy of any particular measurement, whereas the two-wavelength results are more robust over shorter periods. On average, results closely follow the expected diurnal cycle of correlated temperature and humidity during the day and anti-correlated at night. Measured r_{Tq} is approximately 0.6-0.9 in unstable conditions; stable values are more variable but tend to be smaller in magnitude, averaging around -0.3 to -0.5. Observed r_{Tq} was furthest from ±1 during winter and in near neutral conditions. Similar behaviour is seen in r_{Tq_bc} and r_{Tq_EC}, including times when the assumed two-wavelength value will be wrong.

Two-wavelength scintillometer systems have considerable potential to deliver large-area measurements representative of complex environments. Limitations of the two-wavelength method include the ambiguity due to two possible solutions for β and the region of reduced sensitivity around the C_{n2n2} minimum. Research is needed; firstly, to better understand the behaviour in this region and secondly, to investigate improvements to the instrumentation, setup or post-processing to minimise the impact. Advantages of the bichromatic-correlation method include additional information about the atmospheric conditions from r_{Tq_bc}, e.g. the relative sign of the heat fluxes and to what extent MOST conditions are satisfied. For the minimal extra hardware requirements the recommendation is therefore to measure the bichromatic correlation even if the additional information is not used directly in data processing.

The large proportion of vegetation and cool, wet summers helped to maintain a low Bowen ratio in this study. In drier periods or at more built-up sites the results may have been less useable. Future work should focus on the performance of two-wavelength scintillometry under different conditions (notably low crosswind, high Bowen ratio, near neutral stability). Theoretical development (e.g.

modelling studies exploring the impact of differences in footprint and effective height between instruments) combined with careful experimental testing is needed. Comparison data (structure parameters and fluxes) from different methods will be required for thorough evaluation of these techniques.

Acknowledgements

We would like to thank Alan Warwick and Cyril Barrett for constructing the scintillometer mounting brackets, Geoff Wicks for assisting with the electronics and the residents of Swindon who very kindly gave permission for equipment to be installed on their property. We are grateful to Wim Kohsiek and Oscar Hartogensis for their helpful discussions regarding the work presented in Appendix A. This work was funded by the Natural Environment Research Council, UK.

Appendix A. Validity of the small aperture approximation for millimetre-wave scintillometers

The log amplitude of a scintillometer system can be written in a generalised form (e.g. Lüdi et al. 2005),

$$\sigma_{\chi 1 \chi 2} = 4\pi^2 k_1 k_2 0.033 C_n^2 \int_0^\infty dK \int_0^L dx K K^{-11/3} \sin\left(\frac{K^2 x(L-x)}{2k_1 L}\right) \sin\left(\frac{K^2 x(L-x)}{2k_2 L}\right) \times \left[\frac{2J_1(0.5KD_{r1}x/L)}{0.5KD_{r1}x/L}\right]\left[\frac{2J_1(0.5KD_{t1}(1-x/L))}{0.5KD_{t1}(1-x/L)}\right] \times \left[\frac{2J_1(0.5KD_{r2}x/L)}{0.5KD_{r2}x/L}\right]\left[\frac{2J_1(0.5KD_{t2}(1-x/L))}{0.5KD_{t2}(1-x/L)}\right] J_0(K|d|) \quad , \quad \text{(A1)}$$

where $\sigma_{\chi 1 \chi 2}$ is the covariance of log amplitude, C_n^2 the refractive index structure parameter, K the eddy wavenumber and x the position along the path of length L; k is the optical wavenumber, d the beam separation, and D the aperture diameter of the receiver (subscript r) or transmitter (subscript t) for each instrument (subscript 1 or 2) ~~separated by a distance d~~. J_0 and J_1 are Bessel functions of the first kind. The three-dimensional Kolmogorov spectrum $\Phi_n(K) = 0.033 C_n^2 K^{-11/3}$ is assumed.

For a single instrument, this reduces to the standard formula for a large aperture scintillometer (Hill and Ochs 1978):

$$\sigma_\chi^2 = 4\pi^2 k^2 0.033 C_n^2 \int_0^\infty dK \int_0^L dx K K^{-11/3} \sin^2\left(\frac{K^2 x(L-x)}{2kL}\right) \times \left[\frac{2J_1(0.5KD_r x/L)}{0.5KD_r x/L}\right]^2 \left[\frac{2J_1(0.5KD_t(1-x/L))}{0.5KD_t(1-x/L)}\right]^2 . \qquad \text{(A2)}$$

For cases when aperture averaging is unimportant, the standard formula for small aperture scintillometers,

$$\sigma_\chi^2 = 4\pi^2 k^2 0.033 C_n^2 \int_0^\infty dK \int_0^L dx K K^{-11/3} \sin^2\left(\frac{K^2 x(L-x)}{2kL}\right), \qquad \text{(A3)}$$

~~which~~ gives

$$\sigma_\chi^2 = c k^{7/6} L^{11/6} C_n^2 \qquad \text{(A4)}$$

on integration with c = 0.124~~, is often applied~~ (Meijninger et al. 2002a; Lüdi et al. 2005; Meijninger et al. 2006).

Here we consider the validity of applying the small aperture approximation to millimetre-wave, microwave and radiowave systems. For the effects of aperture averaging to be insignificant, the aperture diameter must be sufficiently small compared to the maximal diameter ~~size~~ of the first Fresnel zone, $F = (\lambda L)^{1/2}$. With F around 10 times D, the small aperture approximation causes an appreciable (7%) underestimation of C_n^2 compared to evaluating the full formula (Figure A 1). The relatively long path over Swindon means the difference between formulations is quite small here (3%), but will be more important for shorter paths, shorter wavelengths or larger aperture diameters. Use of the full equation also modifies the path-weighting function slightly; for Swindon the difference in effective heights between using the approximation and full form is 0.15 m.

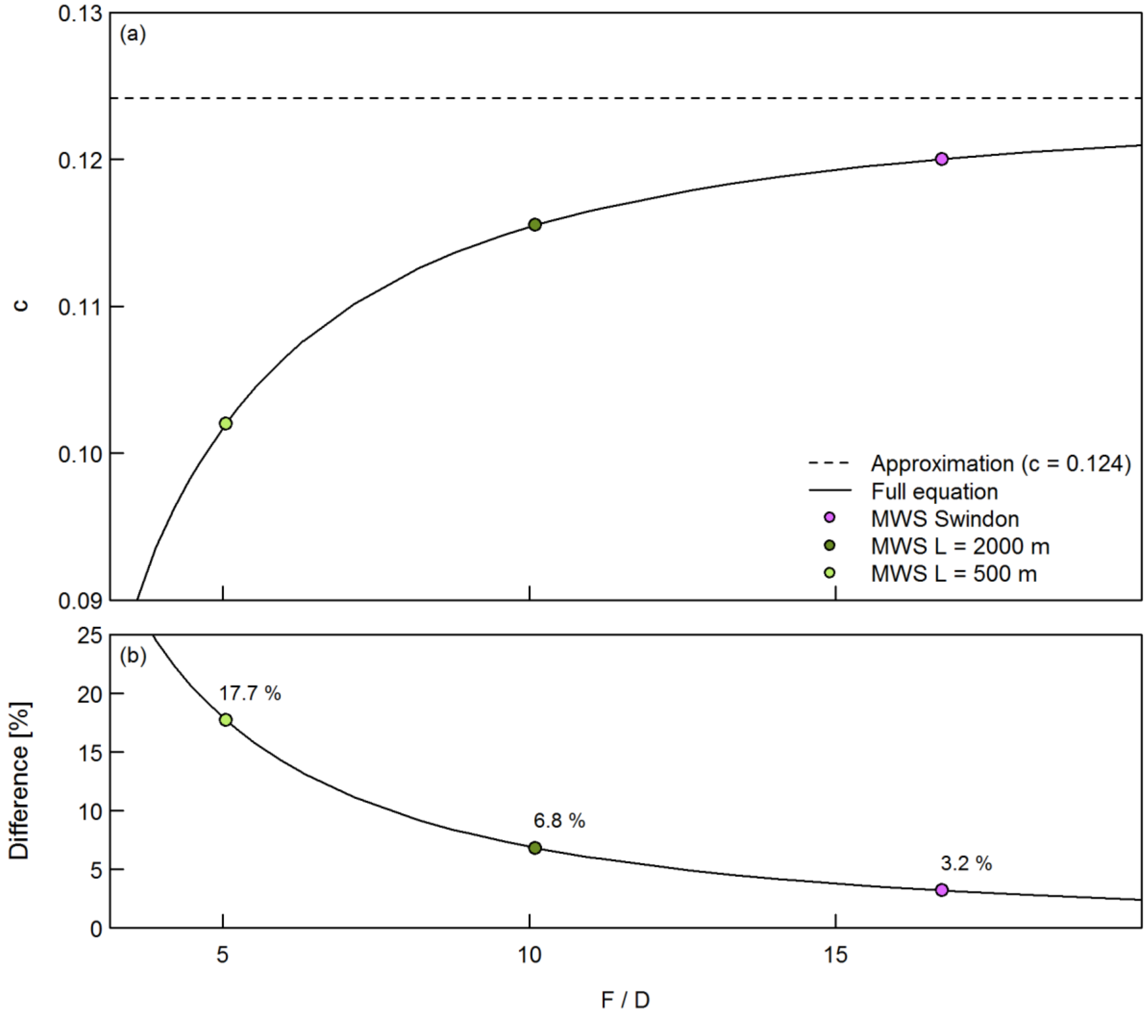

Figure A 1 (a) Value of the multiplier, c, in Equation A4 when calculated using the full equation (Equation A2) as a function of the ratio of Fresnel zone F to aperture diameter D and (b) percentage difference from the small aperture approximation (Equation A3). Some example experimental setups are selected for the CEH-RAL MWS.

References

Allen L, Lindberg F and Grimmond CSB Global to city scale urban anthropogenic heat flux: model and variability. Int J Climatol 31: 1990-2005. doi: 10.1002/joc.2210, 2011.

Andreas EL Estimating C_n^2 over snow and sea ice from meteorological data. J Opt Soc Am 5: 481-495. 1988.

Andreas EL Two-wavelength method of measuring path-averaged turbulent surface heat fluxes. J Atmos Ocean Technol 6: 280-292. 1989.

Andreas EL Three-wavelength method of measuring path-averaged turbulent heat fluxes. J Atmos Ocean Technol 7: 801-814. 1990.

Andreas EL, Hill RJ, Gosz JR, Moore DI, Otto WD and Sarma AD Statistics of surface-layer turbulence over terrain with metre-scale heterogeneity. Boundary-Layer Meteorol 86: 379-408. 1998.

Beyrich F, Bange J, Hartogensis O, Raasch S, Braam M, van Dinther D, Gräf D, van Kesteren B, van den Kroonenberg A, Maronga B, Martin S and Moene A Towards a Validation of

Scintillometer Measurements: The LITFASS-2009 Experiment. Boundary-Layer Meteorol 144: 83-112. doi: 10.1007/s10546-012-9715-8, 2012.

Beyrich F, De Bruin HAR, Meijninger WML, Schipper JW and Lohse H Results from one-year continuous operation of a large aperture scintillometer over a heterogeneous land surface. Boundary-Layer Meteorol 105: 85-97. 2002.

Beyrich F, Kouznetsov RD, Leps JP, Lüdi A, Meijninger WML and Weisensee U Structure parameters for temperature and humidity from simultaneous eddy-covariance and scintillometer measurements. Meteorologische Zeitschrift 14: 641-649. doi: 10.1127/0941-2948/2005/0064, 2005.

Bosveld FC The KNMI Garderen experiment: micro-meteorological observations 1988–1989. KNMI, The Netherlands, 57 pp, 1999.

Braam M Determination of the surface sensible heat flux from the structure parameter of temperature at 60 m height during day-time. KNMI, The Netherlands, 42 pp, 2008.

Braam M, Bosveld F and Moene A On Monin–Obukhov Scaling in and Above the Atmospheric Surface Layer: The Complexities of Elevated Scintillometer Measurements. Boundary-Layer Meteorol 144: 157-177. doi: 10.1007/s10546-012-9716-7, 2012.

Christen A and Vogt R Energy and radiation balance of a central European city. Int J Climatol 24: 1395-1421. doi: 10.1002/joc.1074, 2004.

Clifford SF Temporal-frequency spectra for a spherical wave propagating through atmospheric turbulence. J Opt Soc Am 61: 1285-1292. 1971.

Clifford SF, Ochs GR and Lawrence RS Saturation of optical scintillation by strong turbulence. J Opt Soc Am 64: 148-154. 1974.

De Bruin HAR, Kohsiek W and Van den Hurk BJJM A verification of some methods to determine the fluxes of momentum, sensible heat, and water-vapour using standard-deviation and structure parameter of scalar meteorological quantities. Boundary-Layer Meteorol 63: 231-257. 1993.

Evans JG Long-Path Scintillometry over Complex Terrain to Determine Areal-Averaged Sensible and Latent Heat Fluxes. Soil Science Department, The University of Reading, Reading, UK, PhD Thesis, 181 pp, 2009.

Evans JG and De Bruin HAR The Effective Height of a Two-Wavelength Scintillometer System. Boundary-Layer Meteorol 141: 165-177. doi: 10.1007/s10546-011-9634-0, 2011.

Evans JG, McNeil DD, Finch JF, Murray T, Harding RJ and Verhoef A Evaporation Measurements at Kilometre Scales Determined Using Two-wavelength Scintillometry. BHS Third International Symposium, Role of Hydrology in Managing Consequences of a Changing Global Environment Newcastle University, Newcastle upon Tyne, United Kingdom 19-23 July 2010, 2010.

Evans JG, McNeil DD, Finch JW, Murray T, Harding RJ, Ward HC and Verhoef A Determination of turbulent heat fluxes using a large aperture scintillometer over undulating mixed agricultural terrain. Agric For Meteorol 166-167: 221-233. 2012.

Ezzahar J, Chehbouni A, Hoedjes J, Ramier D, Boulain N, Boubkraoui S, Cappelaere B, Descroix L, Mougenot B and Timouk F Combining scintillometer measurements and an aggregation scheme to estimate area-averaged latent heat flux during the AMMA experiment. J Hydrol 375: 217-226. doi: 10.1016/j.jhydrol.2009.01.010, 2009.

Ezzahar J, Chehbouni A and Hoedjes JCB On the application of scintillometry over heterogeneous grids. J Hydrol 334: 493-501. doi: 10.1016/j.jhydrol.2006.10.027, 2007.

Foken T The energy balance closure problem: An overview. Ecological Applications 18: 1351-1367. 2008.

Garratt JR Transfer characteristics for a heterogeneous surface of large aerodynamic roughness. Q J R Meteorol Soc 104: 491-502. doi: 10.1002/qj.49710444019, 1978.

Garratt JR The Atmospheric Boundary Layer, Cambridge University Press, Cambridge, UK, 316 pp, 1992.

Gouvea ML and Grimmond CSB Spatially integrated measurements of sensible heat flux using scintillometry. Ninth Symposium on the Urban Environment, Keystone, Colorado, 2nd-6th August 2010, 2010.

Green AE, Astill MS, McAneney KJ and Nieveen JP Path-averaged surface fluxes determined from infrared and microwave scintillometers. Agric For Meteorol 109: 233-247. 2001.

Green AE and Hayashi Y Use of the scintillometer technique over a rice paddy. Japanese Journal of Agricultural Meteorology 54: 225-231. 1998.

Grimmond CSB and Oke TR Comparison of Heat Fluxes from Summertime Observations in the Suburbs of Four North American Cities. J Appl Meteorol 34: 873-889. doi: 10.1175/1520-0450(1995)034<0873:COHFFS>2.0.CO;2, 1995.

Grimmond CSB and Oke TR Aerodynamic properties of urban areas derived from analysis of surface form. J Appl Meteorol 38: 1262-1292. 1999.

Grimmond CSB and Oke TR Turbulent heat fluxes in urban areas: Observations and a local-scale urban meteorological parameterization scheme (LUMPS). J Appl Meteorol 41: 792-810. 2002.

Guyot A, Cohard J-M, Anquetin S, Galle S and Lloyd CR Combined analysis of energy and water balances to estimate latent heat flux of a sudanian small catchment. Journal of Hydrology 375: 227-240. 2009.

Hartogensis OK, De Bruin HAR and Van De Wiel BJH Displaced-Beam Small Aperture Scintillometer Test. Part Ii: Cases-99 Stable Boundary-Layer Experiment. Boundary-Layer Meteorol 105: 149-176. doi: 10.1023/a:1019620515781, 2002.

Hartogensis OK, Watts CJ, Rodriguez JC and De Bruin HAR Derivation of an effective height for scintillometers: La Poza experiment in Northwest Mexico. J Hydrometerol 4: 915-928. 2003.

Heusinkveld BG, Jacobs AFG and Holtslag AAM Effect of open-path gas analyzer wetness on eddy covariance flux measurements: A proposed solution. Agric For Meteorol 148: 1563-1573. doi: 10.1016/j.agrformet.2008.05.010, 2008.

Hill RJ Implications of Monin-Obukhov Similarity Theory for Scalar Quantities. Journal of the Atmospheric Sciences 46: 2236-2244. 1989.

Hill RJ Comparison of experiment with a new theory of the turbulence temperature structure-function. Physics of Fluids a-Fluid Dynamics 3: 1572-1576. doi: 10.1063/1.857936, 1991.

Hill RJ Algorithms for obtaining atmospheric surface-layer fluxes from scintillation measurements. J Atmos Ocean Technol 14: 456-467. 1997.

Hill RJ, Bohlander RA, Clifford SF, McMillan RW, Priestly JT and Schoenfeld WP Turbulence-induced millimeter-wave scintillation compared with micrometeorological measurements. IEEE Trans Geosci Remote Sens 26: 330-342. 1988.

Hill RJ, Clifford SF and Lawrence RS Refractive-index and absorption fluctuations in the infrared caused by temperature, humidity, and pressure fluctuations. J Opt Soc Am 70: 1192-1205. 1980.

Hill RJ and Ochs GR Fine calibration of large-aperture optical scintillometers and an optical estimate of inner scale of turbulence. Appl Opt 17: 3608-3612. 1978.

Hoedjes JCB, Zuurbier RM and Watts CJ Large aperture scintillometer used over a homogeneous irrigated area, partly affected by regional advection. Boundary-Layer Meteorol 105: 99-117. 2002.

Kanda M, Moriwaki R, Roth M and Oke T Area-averaged sensible heat flux and a new method to determine zero-plane displacement length over an urban surface using scintillometry. Boundary-Layer Meteorol 105: 177-193. 2002.

Kleissl J, Hartogensis O and Gomez J Test of Scintillometer Saturation Correction Methods Using Field Experimental Data. Boundary-Layer Meteorol 137: 493-507. doi: 10.1007/s10546-010-9540-x, 2010.

Klysik K Spatial and seasonal distribution of anthropogenic heat emissions in Łódź, Poland. Atmos Environ 30: 3397-3404. 1996.

Kohsiek W Measuring C_T^2, C_Q^2, and C_{TQ} in the Unstable Surface-Layer, and Relations to the Vertical Fluxes of Heat and Moisture. Boundary-Layer Meteorol 24: 89-107. 1982.

Kohsiek W and Herben MHAJ Evaporation derived from optical and radio-wave scintillation. Appl Opt 22: 2566-2570. 1983.

Lagouarde JP, Irvine M, Bonnefond JM, Grimmond CSB, Long N, Oke TR, Salmond JA and Offerle B Monitoring the sensible heat flux over urban areas using large aperture scintillometry: Case study of Marseille city during the ESCOMPTE experiment. Boundary-Layer Meteorol 118: 449-476. doi: 10.1007/s10546-005-9001-0, 2006.

Lamaud E and Irvine M Temperature–Humidity Dissimilarity and Heat-to-water-vapour Transport Efficiency Above and Within a Pine Forest Canopy: the Role of the Bowen Ratio. Boundary-Layer Meteorol 120: 87-109. doi: 10.1007/s10546-005-9032-6, 2006.

Leijnse H, Uijlenhoet R and Stricker JNM Hydrometeorological application of a microwave link: 1. Evaporation. Water Resour Res 43: W04416. doi: 10.1029/2006wr004988, 2007.

Li D, Bou-Zeid E and De Bruin HAR Monin-Obukhov Similarity Functions for the Structure Parameters of Temperature and Humidity. Boundary-Layer Meteorol 145: 45-67. doi: 10.1007/s10546-011-9660-y, 2011.

Lüdi A, Beyrich F and Matzler C Determination of the turbulent temperature-humidity correlation from scintillometric measurements. Boundary-Layer Meteorol 117: 525-550. doi: 10.1007/s10546-005-1751-1, 2005.

Medeiros Filho F, Jayasuriya D, Cole R and Helmis C Spectral density of millimeter wave amplitude scintillations in an absorption region. Antennas and Propagation, IEEE Transactions on 31: 672-676. 1983.

Meijninger WML Surface fluxes over natural landscapes using scintillometry. Meteorology and Air Quality Group, Wageningen University, Wageningen, The Netherlands, PhD Thesis, 170 pp, 2003.

Meijninger WML, Beyrich F, Lüdi A, Kohsiek W and De Bruin HAR Scintillometer-based turbulent fluxes of sensible and latent heat over a heterogeneous land surface - A contribution to LITFASS-2003. Boundary-Layer Meteorol 121: 89-110. doi: 10.1007/s10546-005-9022-8, 2006.

Meijninger WML, Green AE, Hartogensis OK, Kohsiek W, Hoedjes JCB, Zuurbier RM and De Bruin HAR Determination of area-averaged water vapour fluxes with large aperture and radio wave scintillometers over a heterogeneous surface - Flevoland field experiment. Boundary-Layer Meteorol 105: 63-83. 2002a.

Meijninger WML, Hartogensis OK, Kohsiek W, Hoedjes JCB, Zuurbier RM and De Bruin HAR Determination of area-averaged sensible heat fluxes with a large aperture scintillometer over a heterogeneous surface - Flevoland field experiment. Boundary-Layer Meteorol 105: 37-62. 2002b.

Mestayer P, Bagga I, Calmet I, Fontanilles G, Gaudin D, Lee JH, Piquet T, Rosant J-M, Chancibault K, Lebouc L, Letellier L, Mosini M-L, Rodriguez F, Rouaud J-M, Sabre M, Tétard Y, Brut A, Selves J-L, Solignac P-A, Brunet Y, Dayau S, Irvine M, Lagouarde J-P, Kassouk Z, Launeau P, Connan O, Defenouillère P, Goriaux M, Hébert D, Letellier B, Mario D, Najjar G, Nerry F, Quentin C, Biron R, Cohard J-M, Galvez J and Klein P The FluxSAP 2010 hydroclimatological experimental campaign over an heterogeneous urban area. 11th EMS Annual Meeting, Berlin, Germany, 12th-16th September 2011, 2011.

Moene A and Schüttemeyer D The Effect of Surface Heterogeneity on the Temperature–Humidity Correlation and the Relative Transport Efficiency. Boundary-Layer Meteorol 129: 99-113. doi: 10.1007/s10546-008-9312-z, 2008.

Moene AF Effects of water vapour on the structure parameter of the refractive index for near-infrared radiation. Boundary-Layer Meteorol 107: 635-653. 2003.

Monin AS and Yaglom AM Statistical Fluid Mechanics: Mechanics of Turbulence, The MIT Press, Cambridge, Massachusetts, 782 pp, 1971.

Nieveen JP, Green AE and Kohsiek W Using a large-aperture scintillometer to measure absorption and refractive index fluctuations. Boundary-Layer Meteorol 87: 101-116. 1998.

Nordbo A, Järvi L, Haapanala S, Moilanen J and Vesala T Intra-City Variation in Urban Morphology and Turbulence Structure in Helsinki, Finland. Boundary-Layer Meteorol 146: 469-496. doi: 10.1007/s10546-012-9773-y, 2013.

Offerle B, Grimmond CSB and Fortuniak K Heat storage and anthropogenic heat flux in relation to the energy balance of a central European city centre. Int J Climatol 25: 1405-1419. doi: 10.1002/joc.1198, 2005.

Oke TR Boundary Layer Climates, Routledge, Taylor and Francis Group, London, UK, 435 pp, 1987.

Oke TR, Spronken-Smith RA, Jáuregui E and Grimmond CSB The energy balance of central Mexico City during the dry season. Atmos Environ 33: 3919-3930. 1999.

Otto WD, Hill RJ, Sarma AD, Wilson JJ, Andreas EL, Gosz JR and Moore DI Results of the Millimeter-Wave Instrument Operated at Sevilleta, New Mexico. NOAA-TM-ERL-ETL-262, NOAA Environmental Reasearch Laboratories, Boulder, Colorado, 47 pp, 1996.

Pasquill F Atmospheric Diffusion, Wiley, New York, 429 pp, 1974.

Pauscher L Scintillometer Measurements above the Urban Area of London. Department of Micrometeorology, University of Bayreuth, Bayreuth, Germany, 104 pp, 2010.

Poggio LP, Furger M, Prevot ASH, Graber WK and Andreas EL Scintillometer wind measurements over complex terrain. J Atmos Ocean Technol 17: 17-26. 2000.

Ramamurthy P and Bou-Zeid E Contribution of impervious surfaces to urban evaporation. Water Resour Res 50: 2889-2902. doi: 10.1002/2013WR013909, 2014.

Raupach MR, Antonia RA and Rajagopalan S Rough-Wall Turbulent Boundary Layers. Applied Mechanics Reviews 44: 1-25. 1991.

Roth M Turbulent transfer relationships over an urban surface. II: Integral statistics. Q J R Meteorol Soc 119: 1105-1120. doi: 10.1002/qj.49711951312, 1993.

Roth M, Salmond JA and Satyanarayana ANV Methodological considerations regarding the measurement of turbulent fluxes in the urban roughness sublayer: The role of scintillometery. Boundary-Layer Meteorol 121: 351-375. doi: 10.1007/s10546-006-9074-4, 2006.

Samain B, Defloor W and Pauwels VRN Continuous Time Series of Catchment-Averaged Sensible Heat Flux from a Large Aperture Scintillometer: Efficient Estimation of Stability Conditions and Importance of Fluxes under Stable Conditions. J Hydrometerol 13: 423-442. doi: 10.1175/jhm-d-11-030.1, 2012a.

Samain B, Simons GWH, Voogt MP, Defloor W, Bink N-J and Pauwels VRN Consistency between hydrological model, large aperture scintillometer and remote sensing based evapotranspiration estimates for a heterogeneous catchment. Hydrol Earth Syst Sci 16: 2095-2107. doi: 10.5194/hess-16-2095-2012, 2012b.

Schotanus P, Nieuwstadt FTM and Bruin HAR Temperature measurement with a sonic anemometer and its application to heat and moisture fluxes. Boundary-Layer Meteorol 26: 81-93. doi: 10.1007/bf00164332, 1983.

Scintec Scintec Boundary Layer Scintillometer Hardware Manual. Rottenburg, Germany: 67, 2009.

Solignac PA, Brut A, Selves JL, Béteille JP and Gastellu-Etchegorry JP Attenuating the Absorption Contribution on {C_{n^{2}}} Estimates with a Large-Aperture Scintillometer. Boundary-Layer Meteorol 143: 261-283. doi: 10.1007/s10546-011-9692-3, 2012.

Solignac PA, Brut A, Selves JL, Beteille JP, Gastellu-Etchegorry JP, Keravec P, Beziat P and Ceschia E Uncertainty analysis of computational methods for deriving sensible heat flux values from scintillometer measurements. Atmospheric Measurement Techniques 2: 741-753. 2009.

Stull RB An Introduction to Boundary Layer Meteorology, Kluwer Academic Publishers, Dordrecht, The Netherlands, 666 pp, 1988.

Tatarski VI Wave Propagation in a Turbulent Medium, McGraw-Hill, New York, 285 pp, 1961.

Van Kesteren AJH Sensible and Latent Heat Fluxes with Optical and Millimetre Wave Scintillometers: A Theory Review and the Chilbolton Experiment. Wageningen University, Wageningen, The Netherlands, Masters Thesis, 99 pp, 2008.

Von Randow C, Kruijt B, Holtslag AAM and de Oliveira MBL Exploring eddy-covariance and large-aperture scintillometer measurements in an Amazonian rain forest. Agric For Meteorol 148: 680-690. doi: 10.1016/j.agrformet.2007.11.011, 2008.

Wang TI, Ochs GR and Clifford SF A saturation-resistant optical scintillometer to measure C_n^2. J Opt Soc Am 68: 334-338. 1978.

Wang TI, Ochs GR and Lawrence RS Wind measurements by the temporal cross-correlation of the optical scintillations. Appl Opt 20: 4073-4081. 1981.

Ward HC, Evans JG and Grimmond CSB Effects of Non-Uniform Crosswind Fields on Scintillometry Measurements. Boundary-Layer Meteorol 141: 143-163. doi: 10.1007/s10546-011-9626-0, 2011.

Ward HC, Evans JG and Grimmond CSB Multi-season eddy covariance observations of energy, water and carbon fluxes over a suburban area in Swindon, UK. Atmos Chem Phys 13: 4645-4666. doi: 10.5194/acp-13-4645-2013, 2013a.

Ward HC, Evans JG and Grimmond CSB Infrared and millimetre-wave scintillometry in the suburban environment – Part 2: Large-area sensible and latent heat fluxes. Atmospheric Measurement Techniques Discussions 7: 11221-11264. 2014a.

Ward HC, Evans JG and Grimmond CSB Multi-scale sensible heat fluxes in the urban environment from large aperture scintillometry and eddy covariance. Boundary Layer Meteorol 152: 65-89. doi: 10.1007/s10546-014-9916-4, 2014b.

Ward HC, Evans JG, Hartogensis OK, Moene AF, De Bruin HAR and Grimmond CSB A critical revision of the estimation of the latent heat flux from two-wavelength scintillometry. Q J R Meteorol Soc 139: 1912-1922. doi: 10.1002/qj.2076, 2013b.

Wesely ML Combined effect of temperature and humidity fluctuations on refractive-index. J Appl Meteorol 15: 43-49. 1976.

Wood CR, Kouznetsov RD, Gierens R, Nordbo A, Järvi L, Kallistratova MA and Kukkonen J On the Temperature Structure Parameter and Sensible Heat Flux over Helsinki from Sonic Anemometry and Scintillometry. J Atmos Ocean Technol 30: 1604-1615. doi: 10.1175/JTECH-D-12-00209.1, 2013.

Wood N and Mason P The influence of static stability on the effective roughness lengths for momentum and heat transfer. Q J R Meteorol Soc 117: 1025-1056. doi: 10.1002/qj.49711750108, 1991.

Zieliński M, Fortuniak K, Pawlak Wo and Siedlecki M Turbulent sensible heat flux in Łódź, Central Poland, obtained from scintillometer and eddy covariance measurements. Meteorologische Zeitschrift 22: 603-613. 2013.